The LTP interferometer and Phasemeter

G Heinzel[a], V Wand[a], A Marin[a], C Braxmaier[b], R Schilling[a], A Rüdiger[a], D Robertson[c], O Jennrich[d], U Johann[b] and K Danzmann[a]

[a] Max-Planck-Institut für Gravitationsphysik (Albert-Einstein-Institut), Callinstrasse 38, D-30167 Hannover, Germany.

[b] Astrium GmbH, 88039 Friedrichshafen, Germany

[c] Dept. of Physics and Astronomy, University of Glasgow, UK

[d] ESTEC, Noordwijk, The Netherlands

Journées du GREX 2004,
Nice 28/10/2004.

Heterodyne Mach-Zehnder interferometer

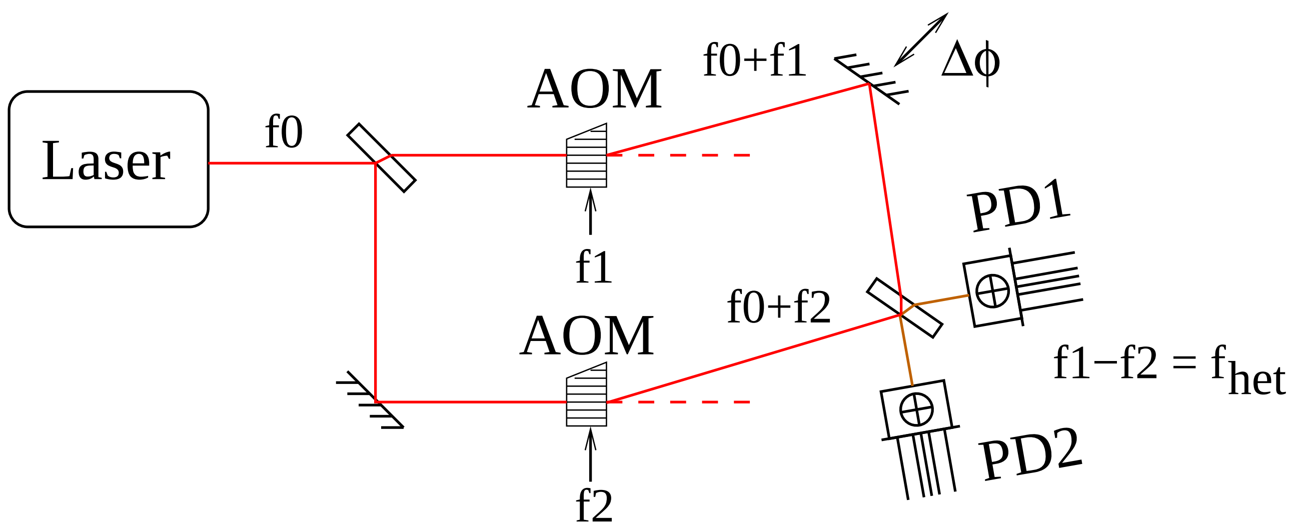

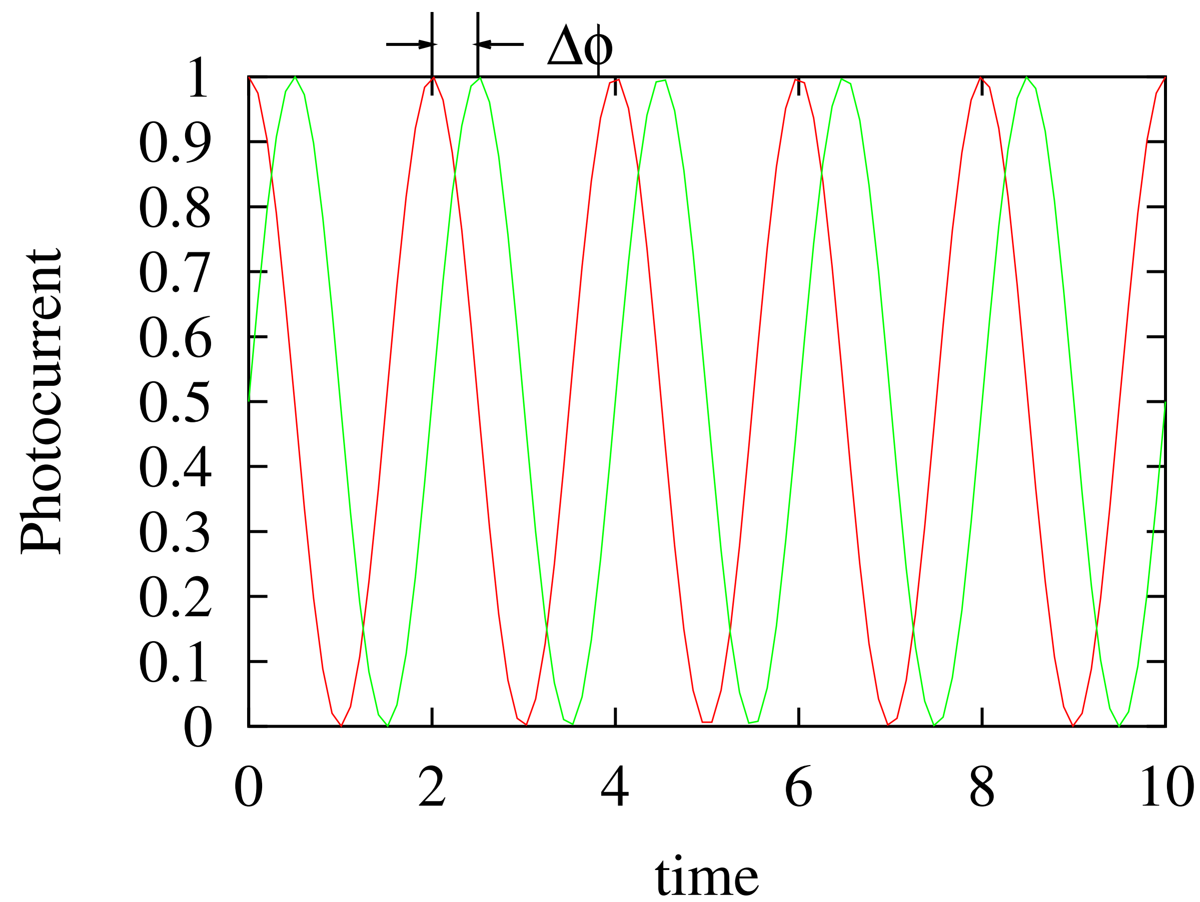

It has constant sensitivity over a range of $> \pm 100\,\mu$m. The heterodyne frequency f_{het} is a few kHz (1.6 kHz in the EM).

Interferometer budget

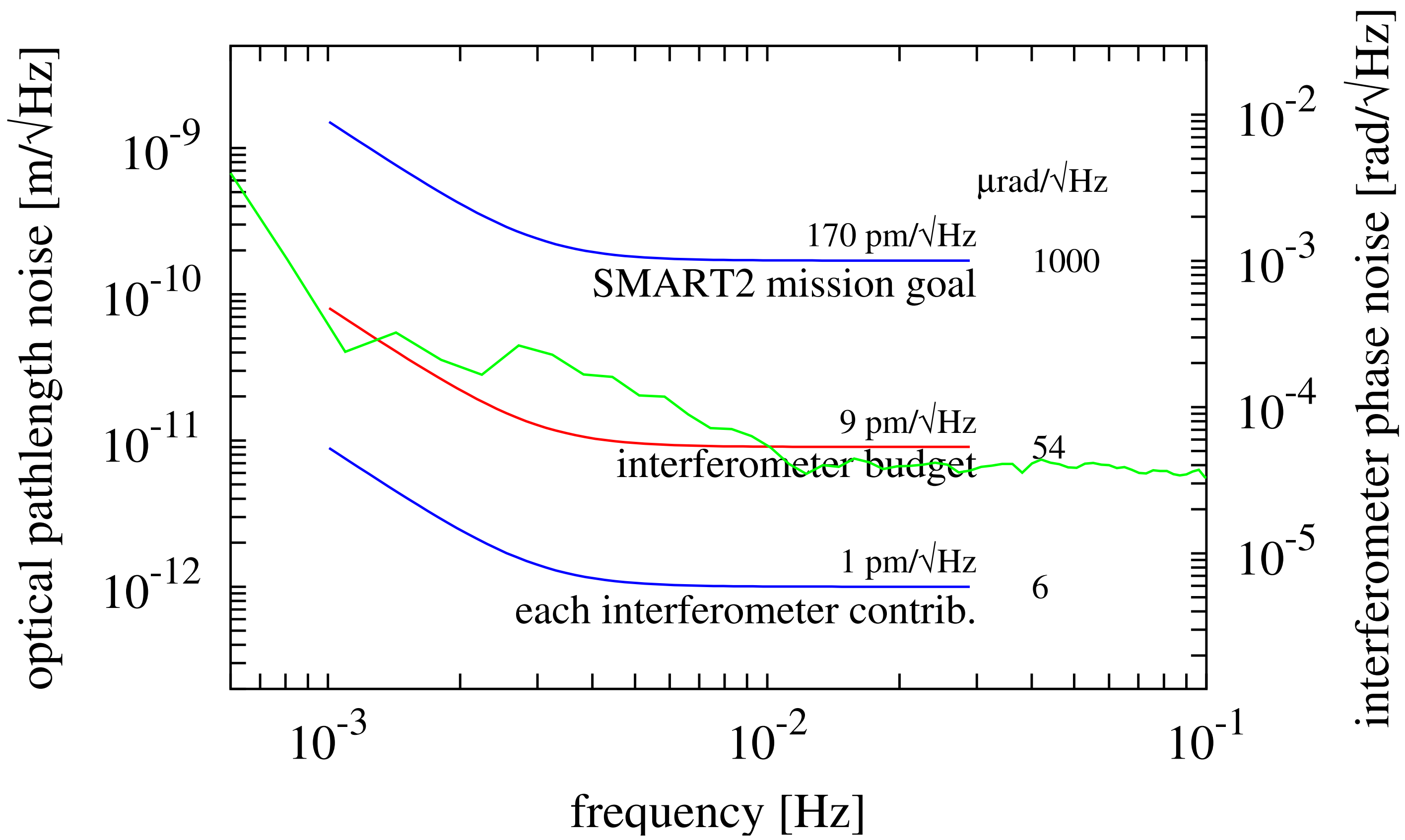

The frequency dependence of all interferometer-related budgets is

$$y(f) = y(30\,\text{mHz}) \cdot \sqrt{1 + \left(\frac{3\,\text{mHz}}{f}\right)^4}\,,$$

and all budgets in the following are given at 30 mHz (such as $9\,\text{pm}/\sqrt{\text{Hz}}$ for the interferometer).

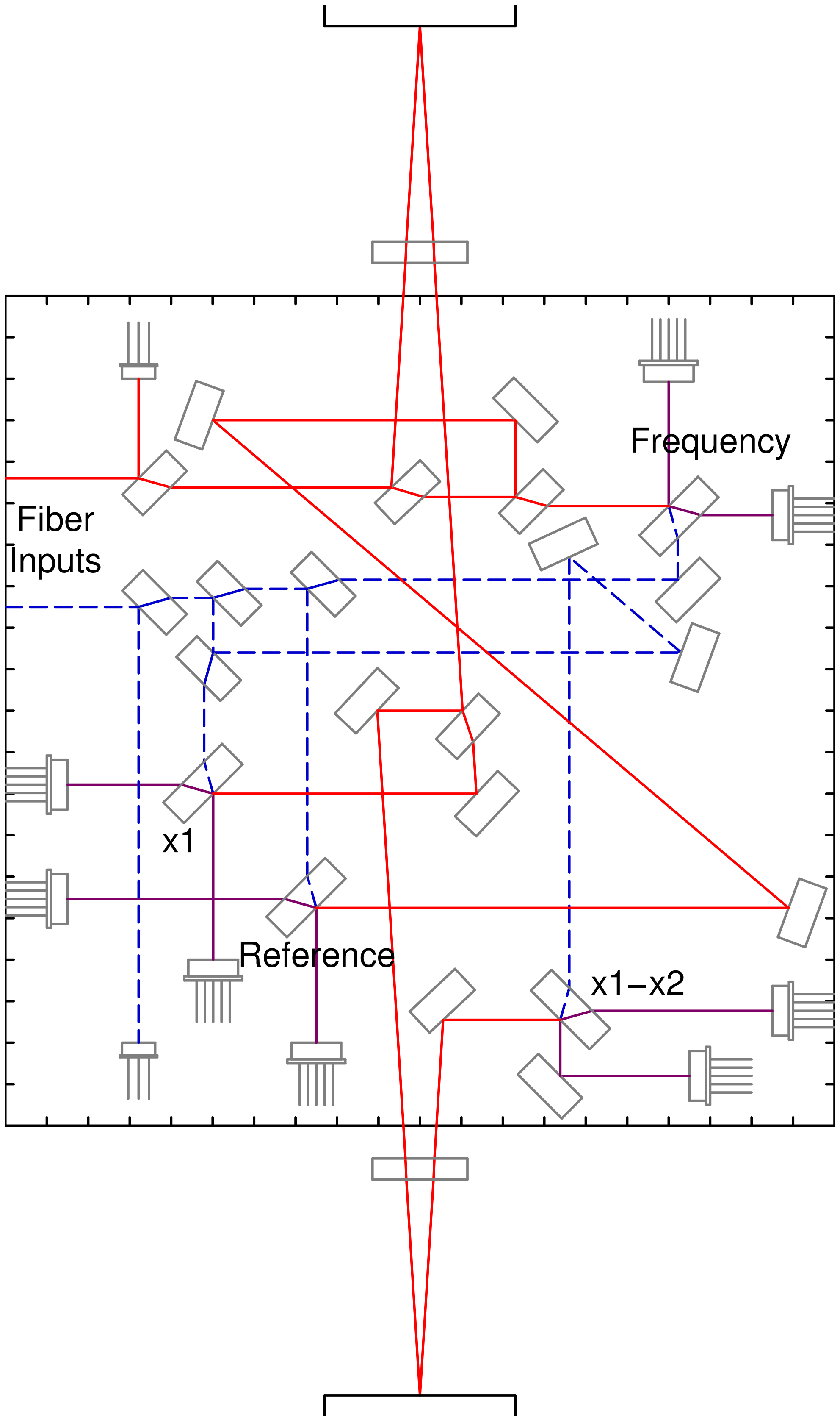

4 interferometers:

$x_1 - x_2$ provides the main measurement: the distance between the two test masses and their differential alignment.

x_1 provides as auxiliary measurement the distance between one test mass and the optical bench and the alignment of that test mass.

Reference provides the reference phase for $x_1 - x_2$ and x_1.

Frequency measures laser frequency fluctuations with intentionally unequal pathlengths.

$x_1 - x_2$

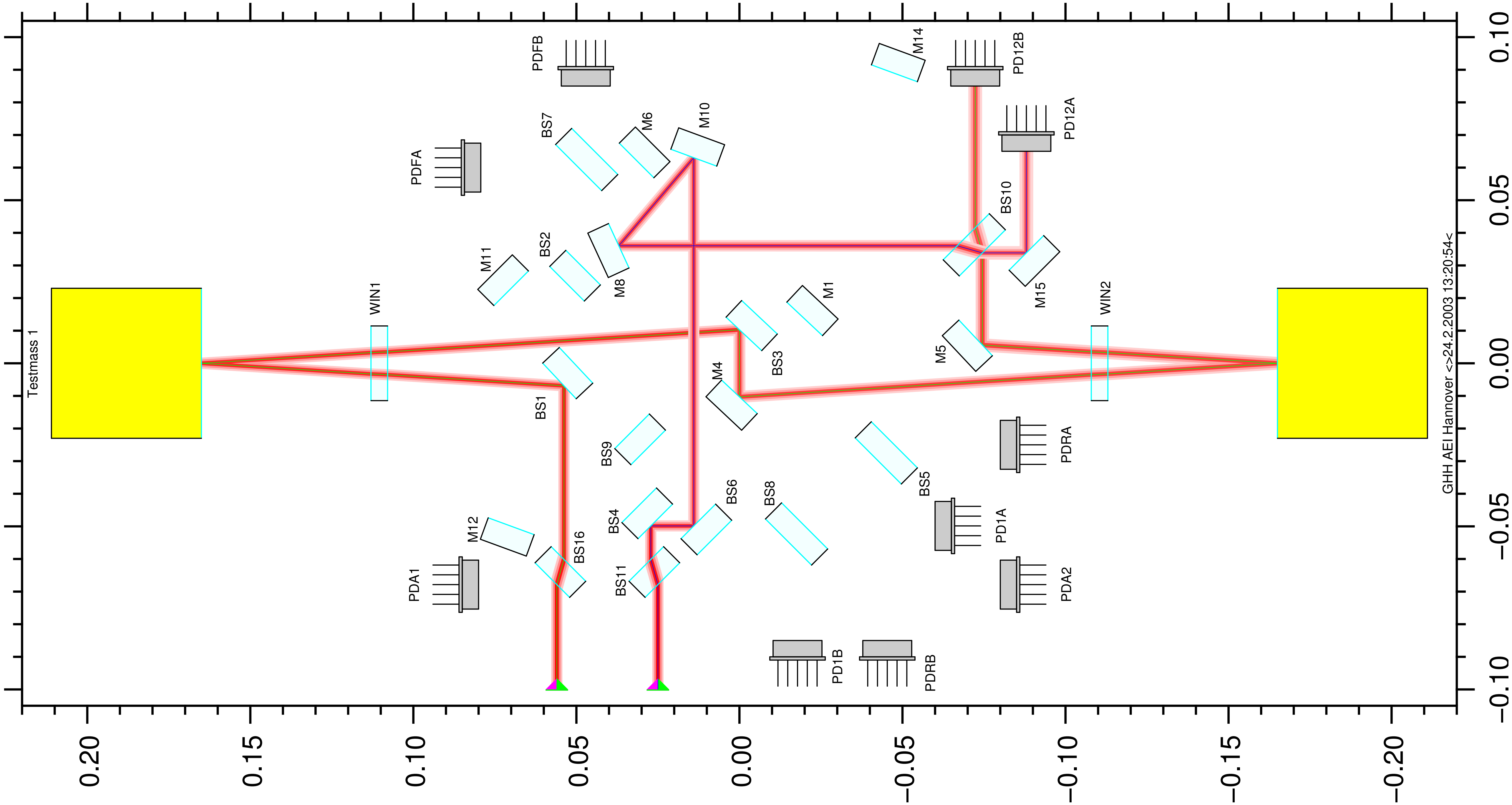

with an extra pathlength of 356.7 mm in the reference fiber, the pathlength difference is 0.000 mm.

x_1

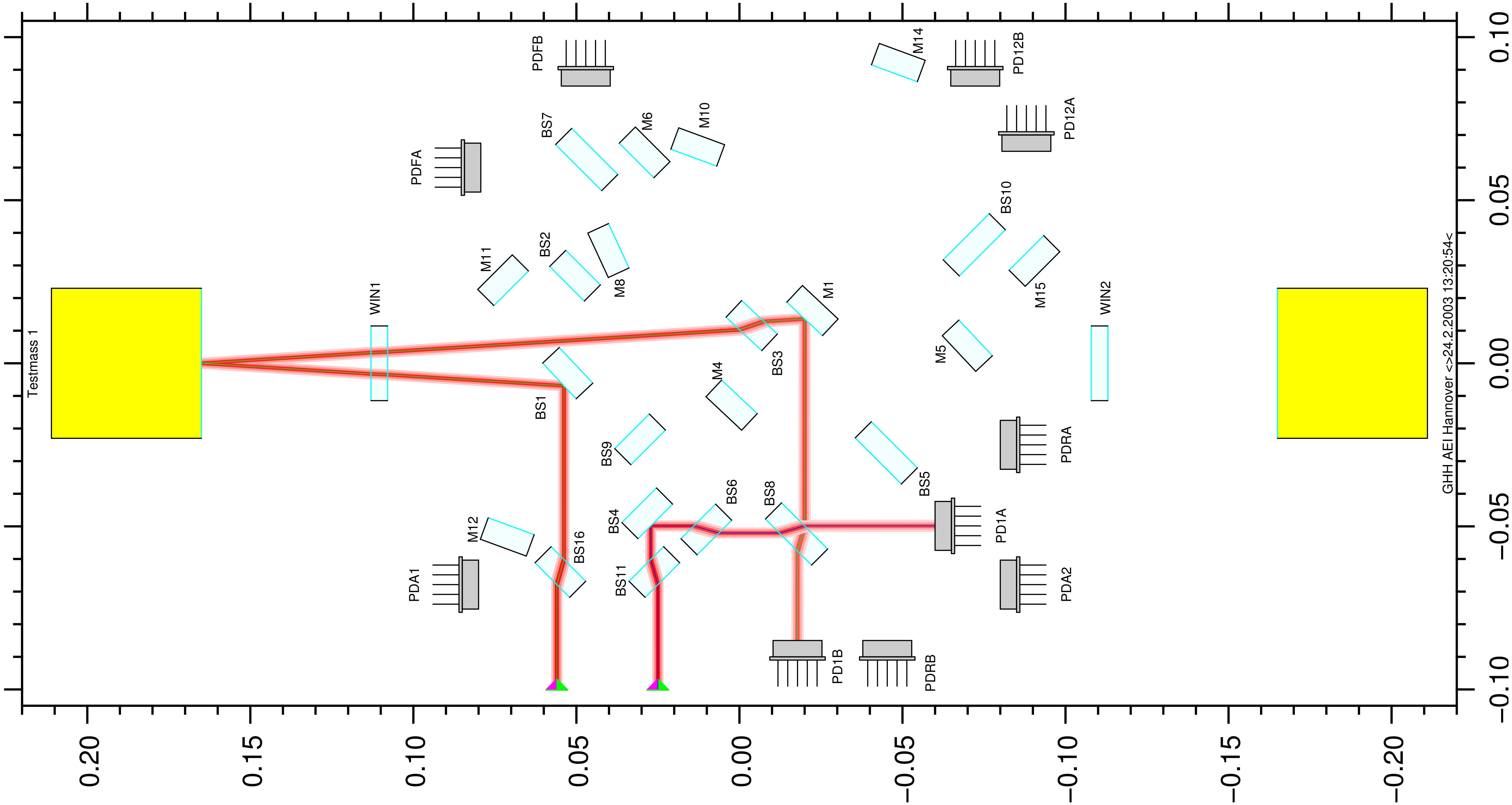

with an extra pathlength of 356.7 mm in the reference fiber, the pathlength difference is 0.02 mm.

Reference

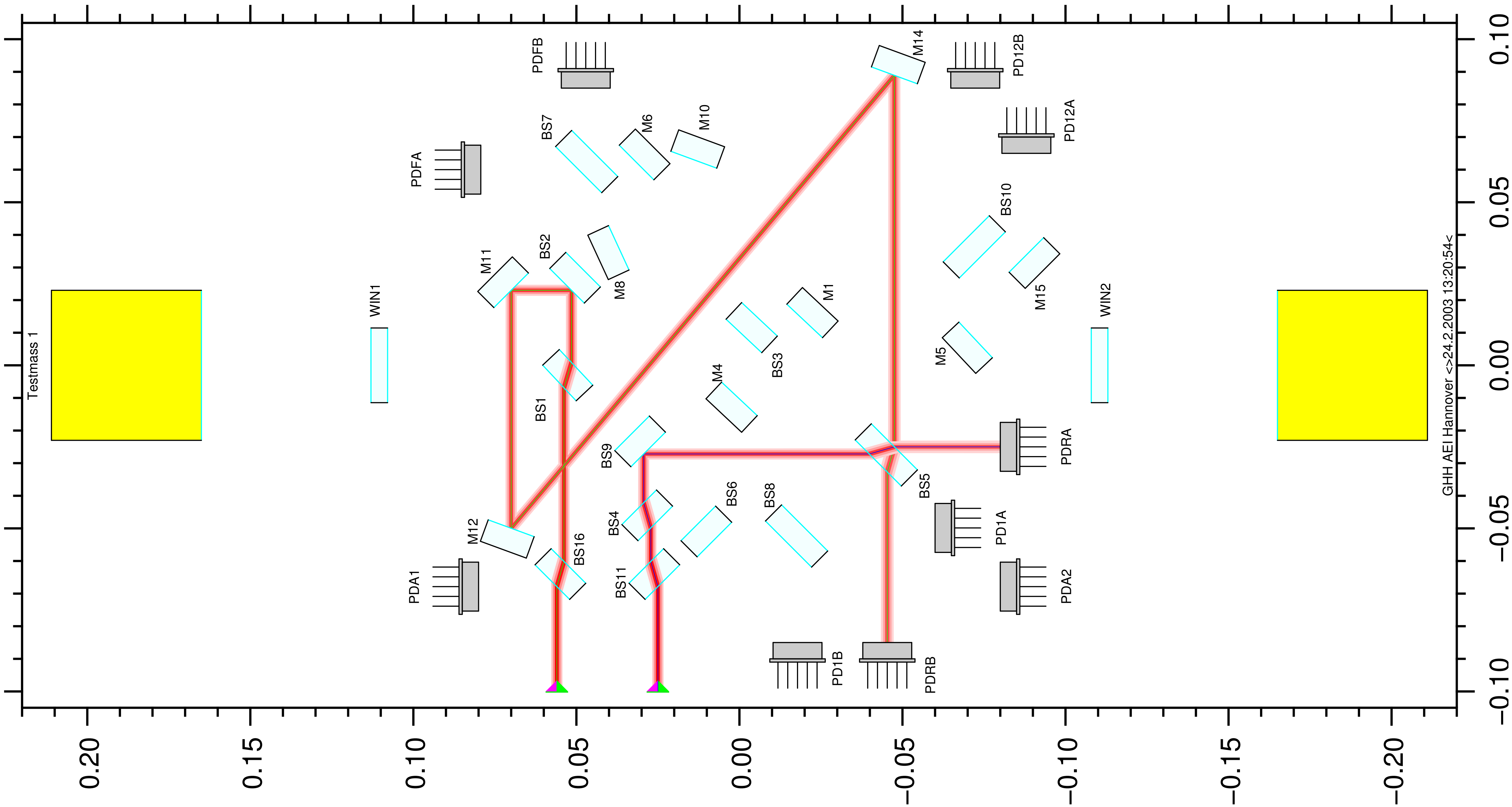

with an extra pathlength of 356.7 mm in the reference fiber, the pathlength difference is 0.016 mm.

Frequency

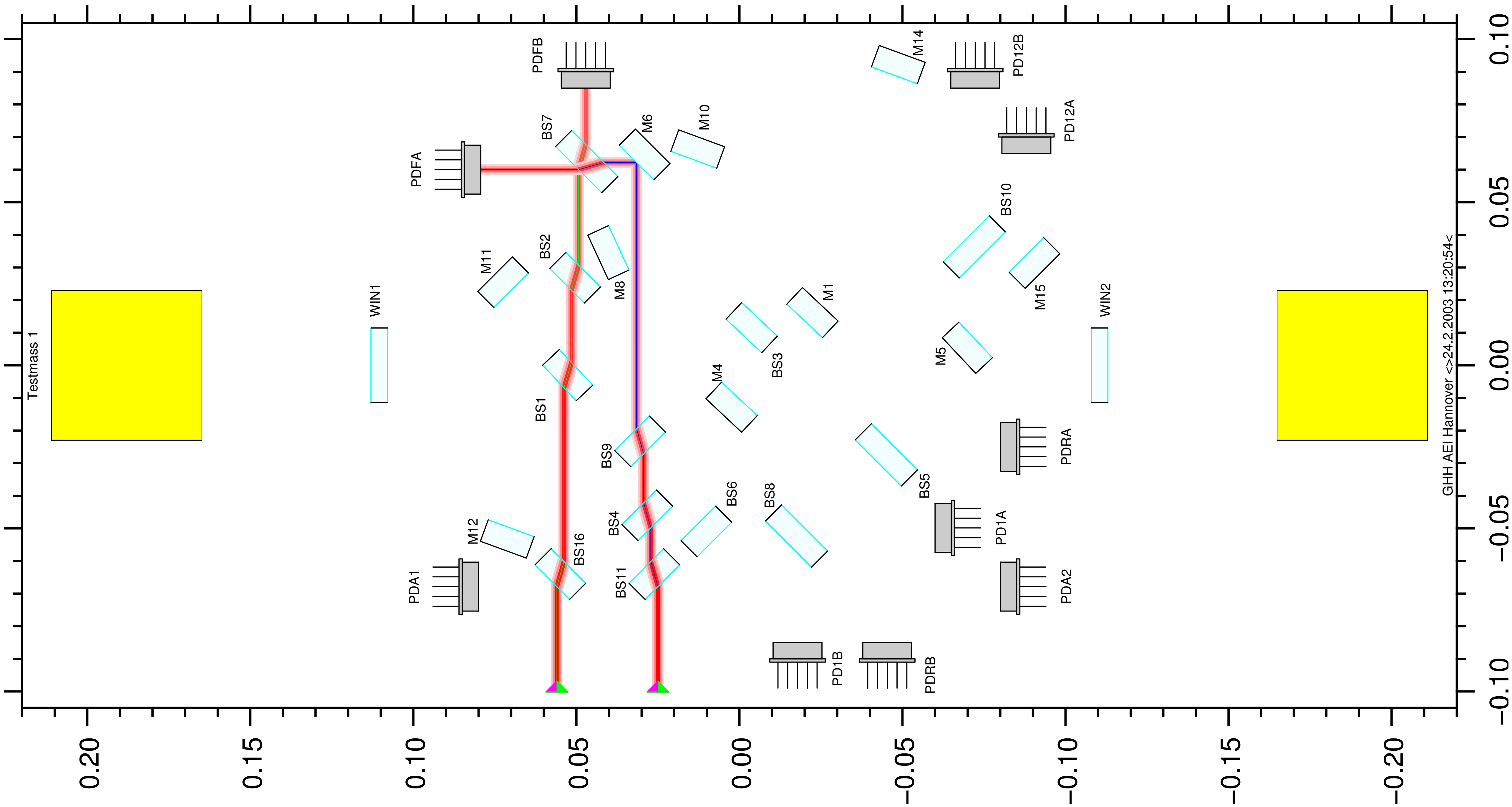

with an extra pathlength of 356.7 mm in the reference fiber, the pathlength difference is −380 mm.

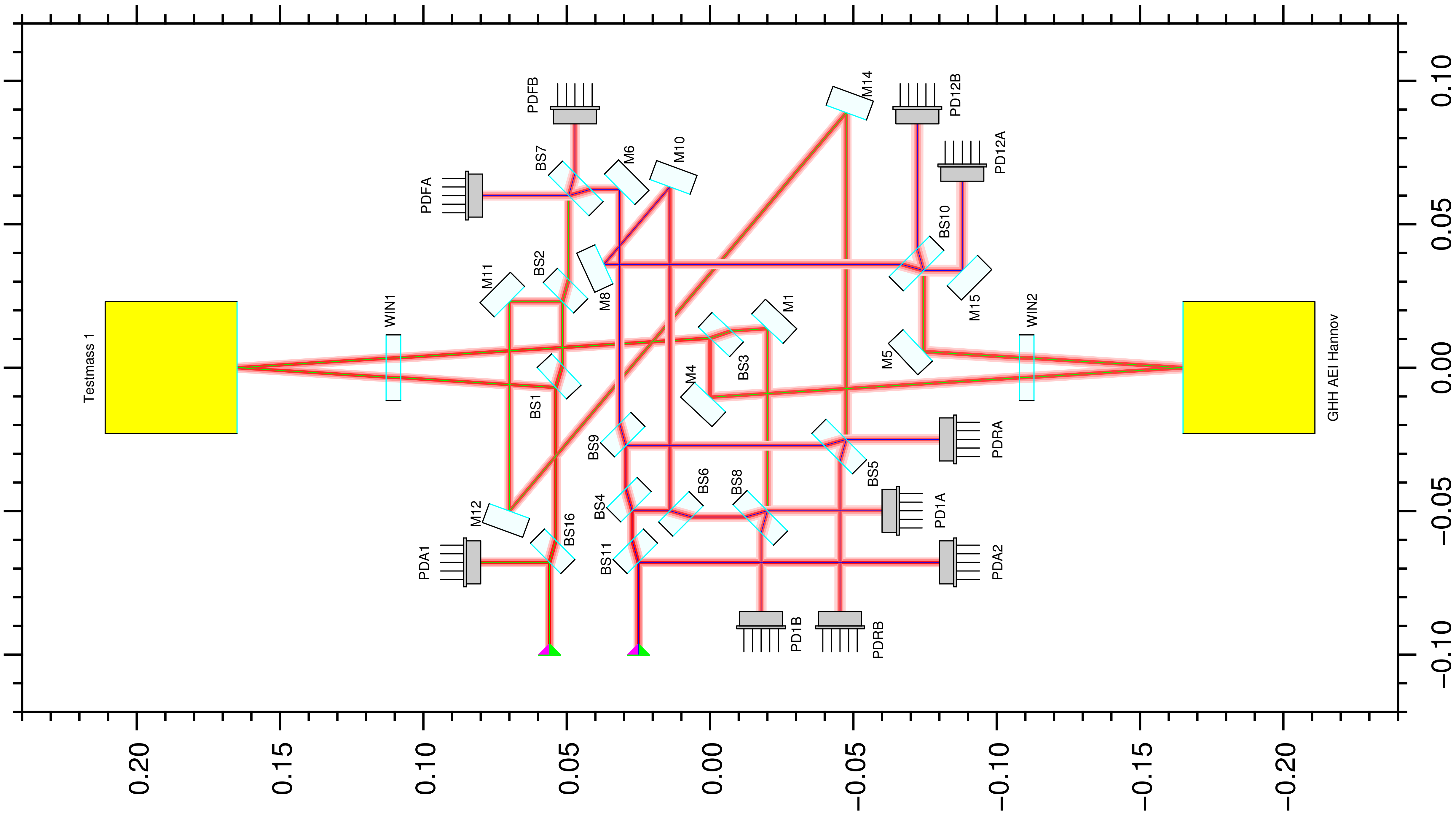

Testmass 1
WIN1
M11
BS2
BS7
PDFB
PDFA
M6
M10
M8
M14
PD12B
PD12A
BS10
M15
WIN2
M1
BS3
M4
M5
BS1
BS9
BS5
PDRA
BS4
BS6
BS8
PD1A
M12
BS16
BS11
PDA1
PDA2
PD1B
PDRB
GHH AEI Hannov
0.20
0.15
0.10
0.05
0.00
−0.05
−0.10
−0.15
−0.20

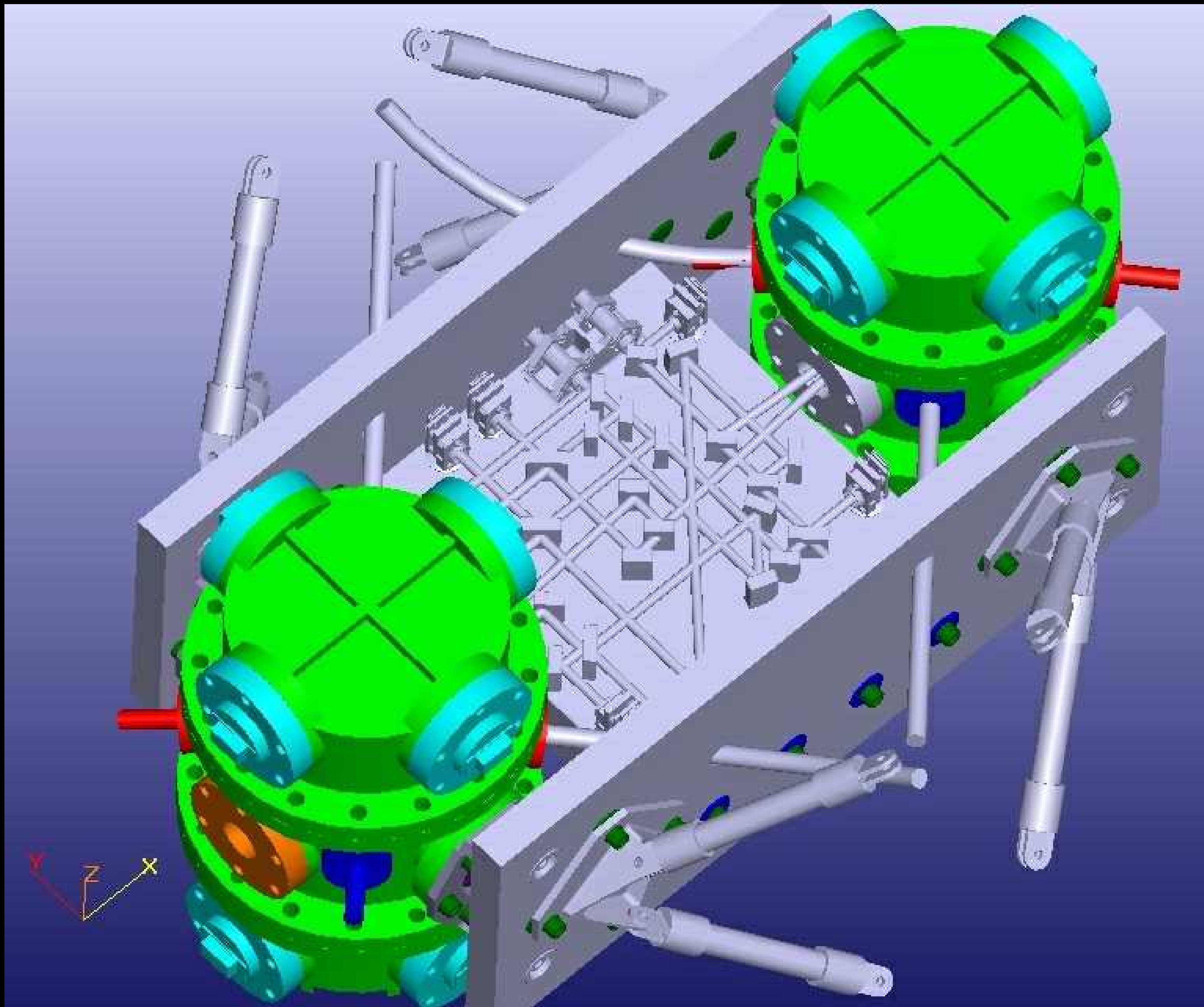
Y
Z
X

Optical bench manufacturing

The OB was manufactured by RAL from a Zerodur baseplate and fused silica optical components, using hydroxycatalysis bonding from U Glasgow and the optical design from AEI.

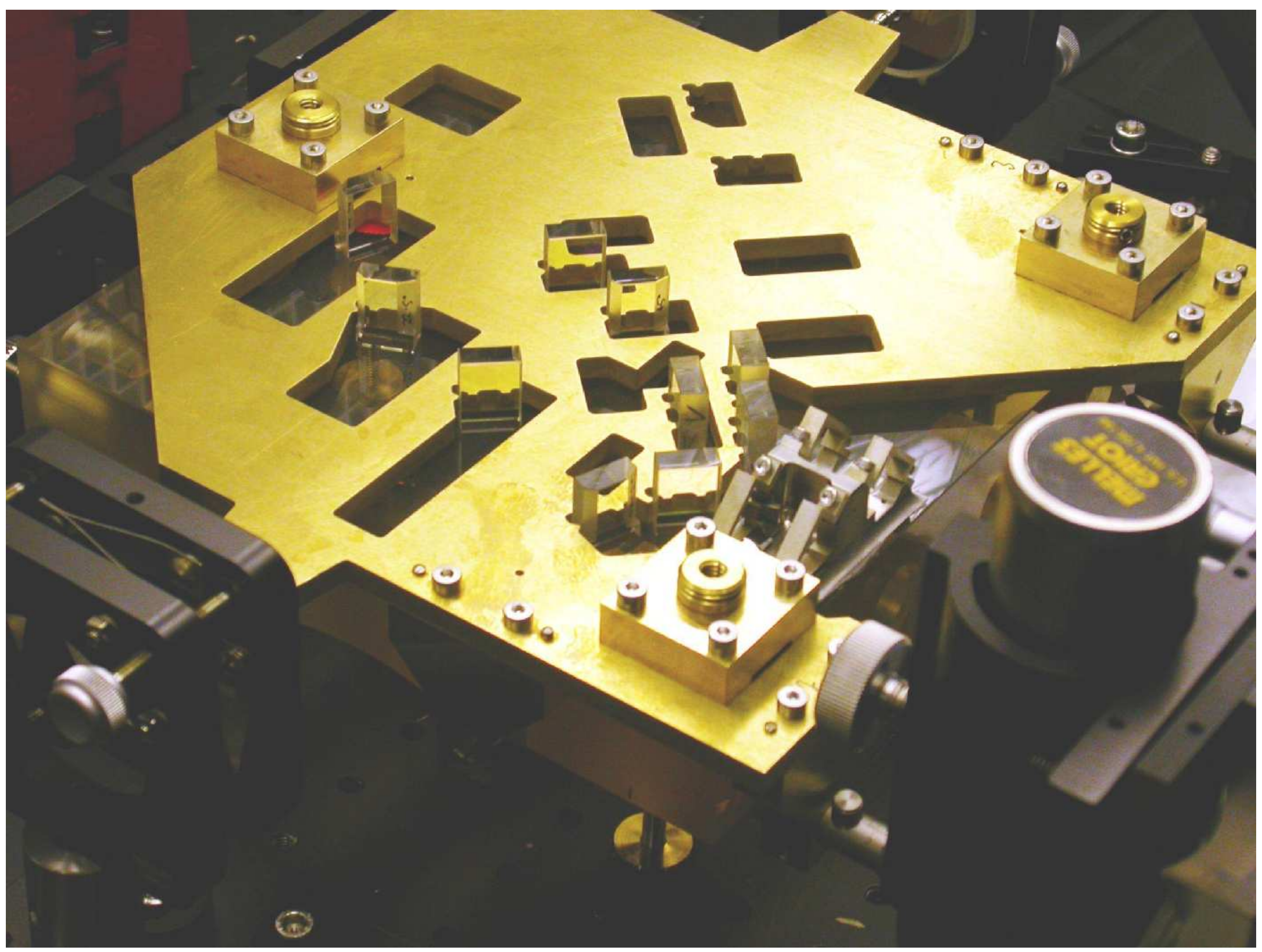

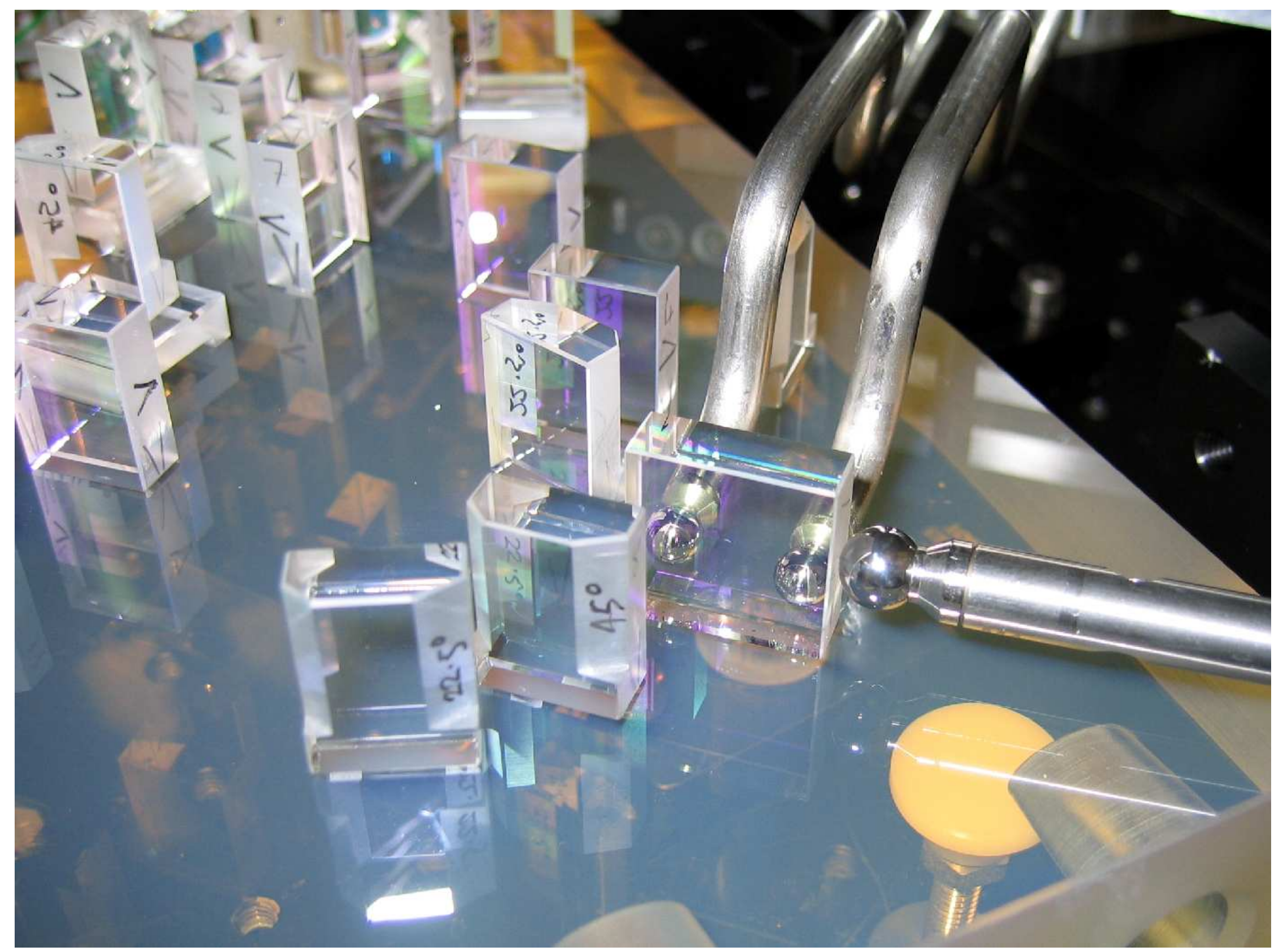

Recovery from accident

A handling mistake caused 4 components to break at a late assembly stage. They could be repaired with interface plates ('bridges').

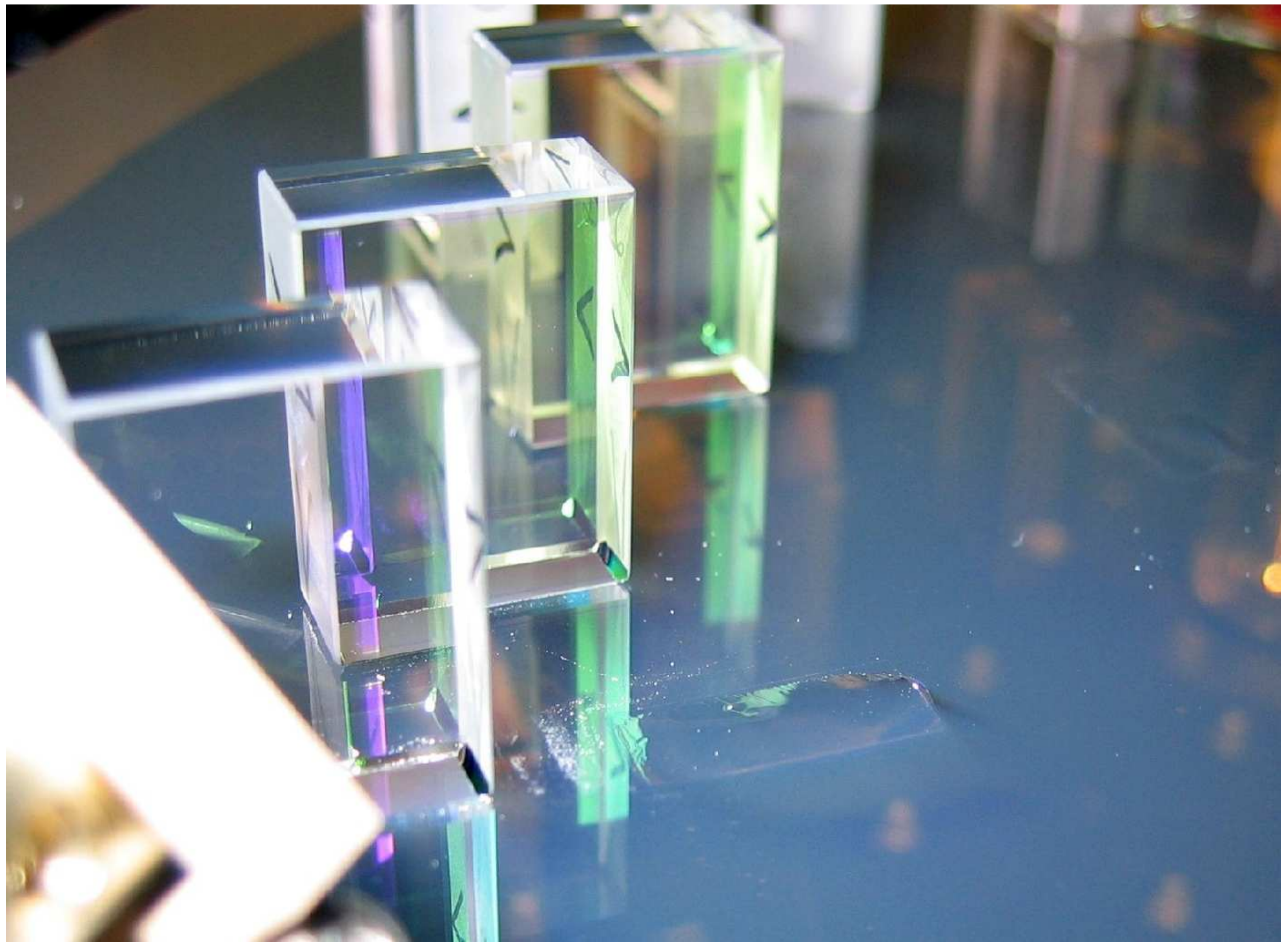

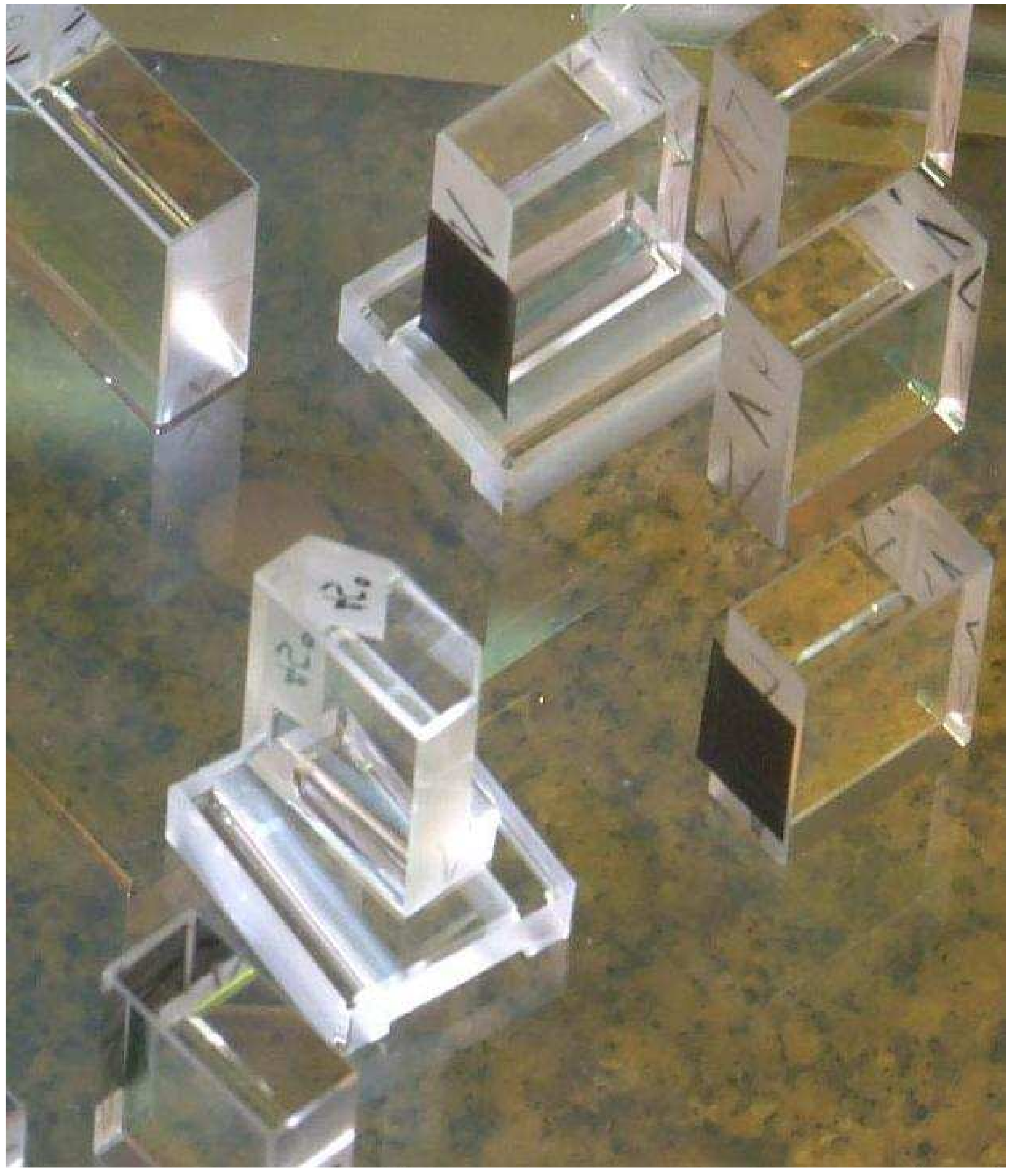


EADS
ASTRIUM
Albert-Einstein-Institut Hannover

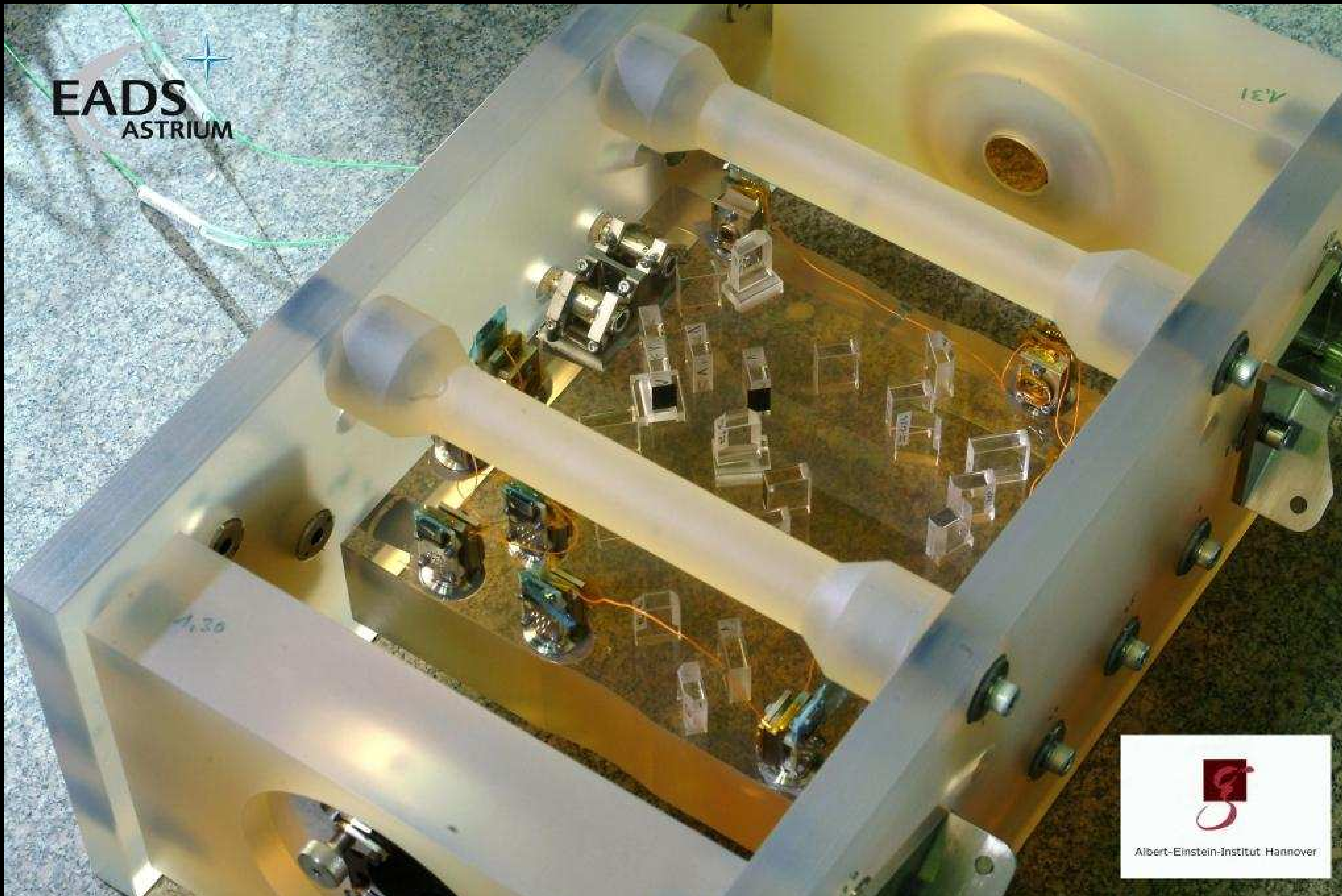
EADS
ASTRIUM
Albert-Einstein-Institut Hannover

Laser source

The laser (by Tesat) is already space qualified and delivers 25 mW at the end of an optical fiber.

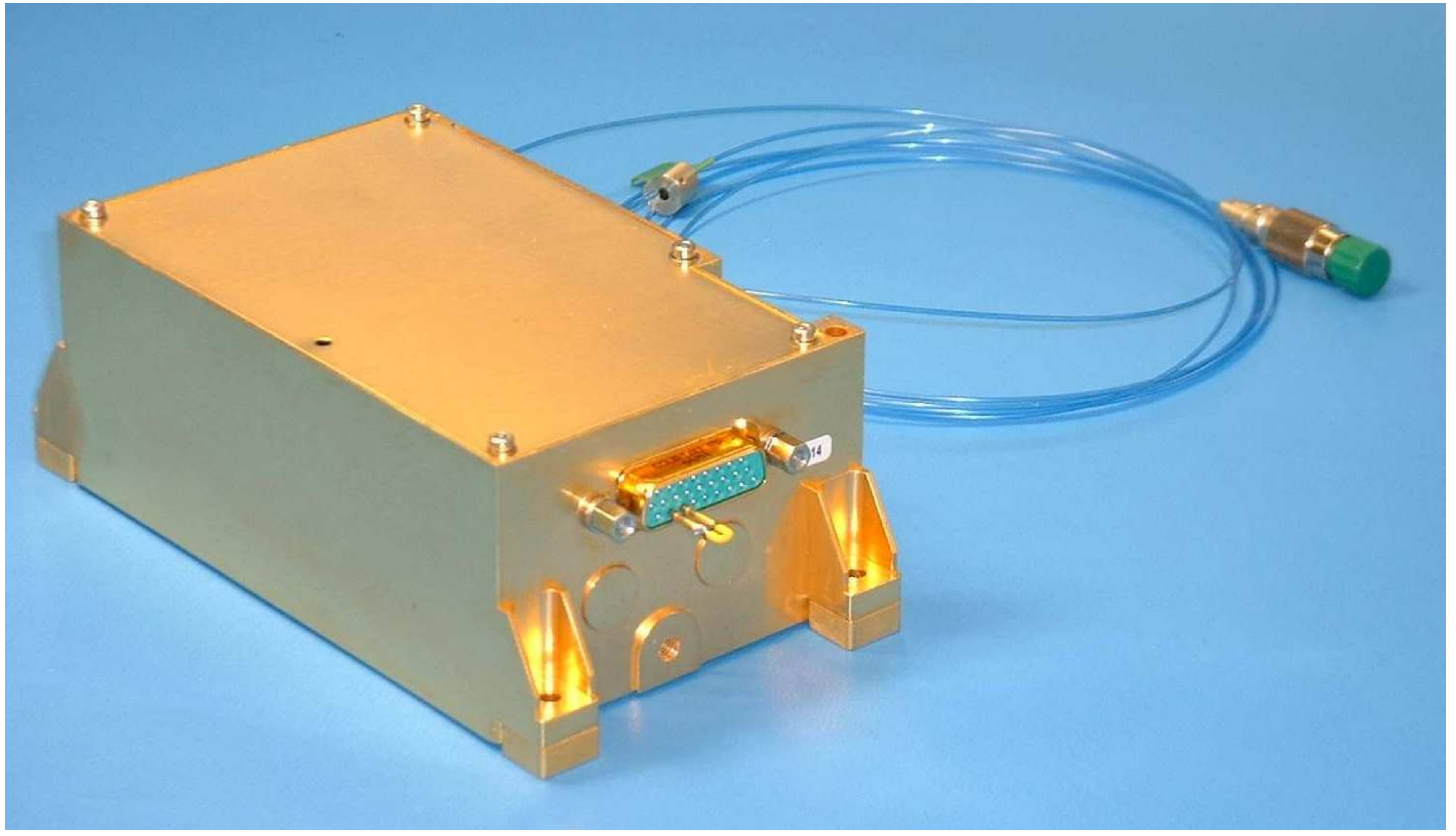

It will be included in a larger box together with the Acousto optical modulators and associated electronics.

AOM Prototype (Contraves)

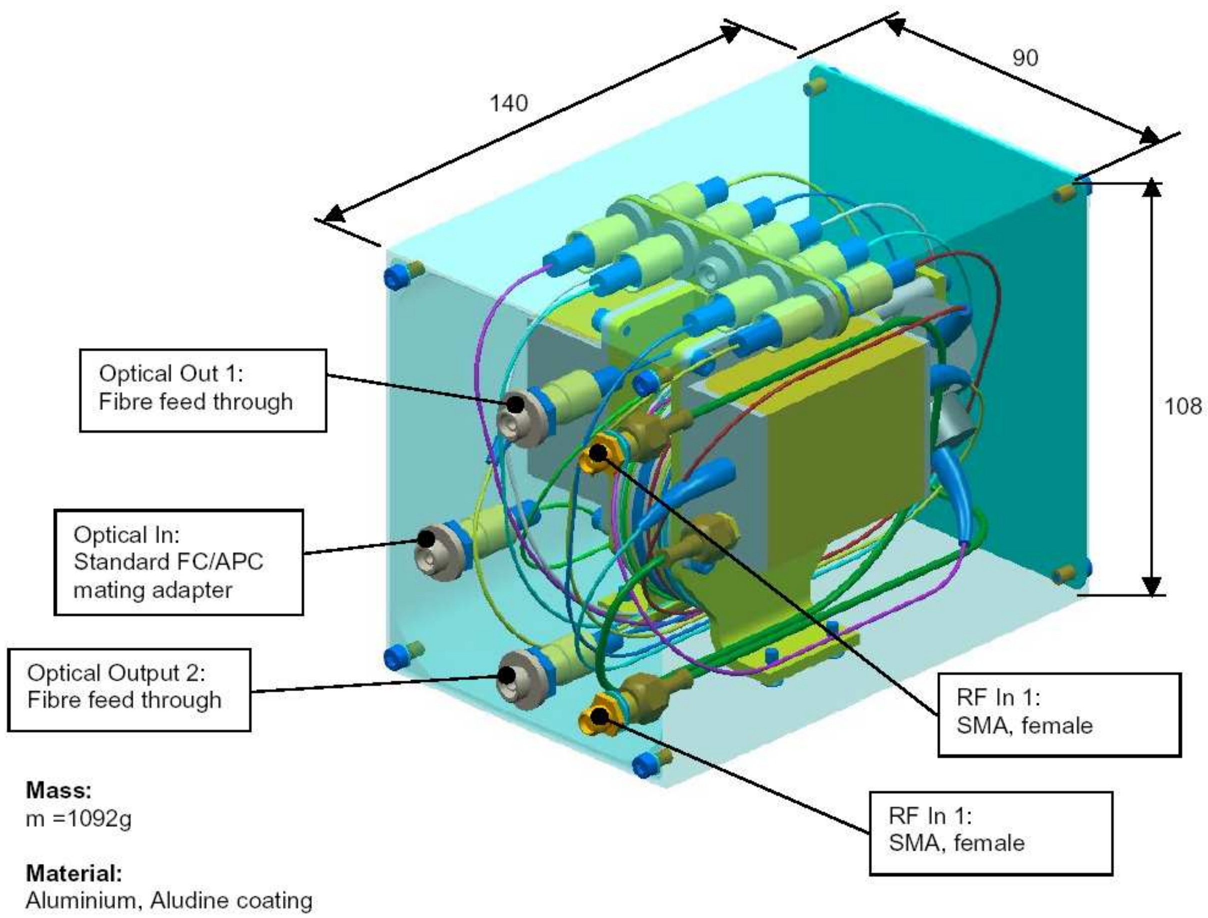

3D-plot of the mechanical layout of the Modulation Bench

Note: The figure shows FC/APC mating adapters for the outputs; To avoid losses these are substituted by fibre feed throughs.

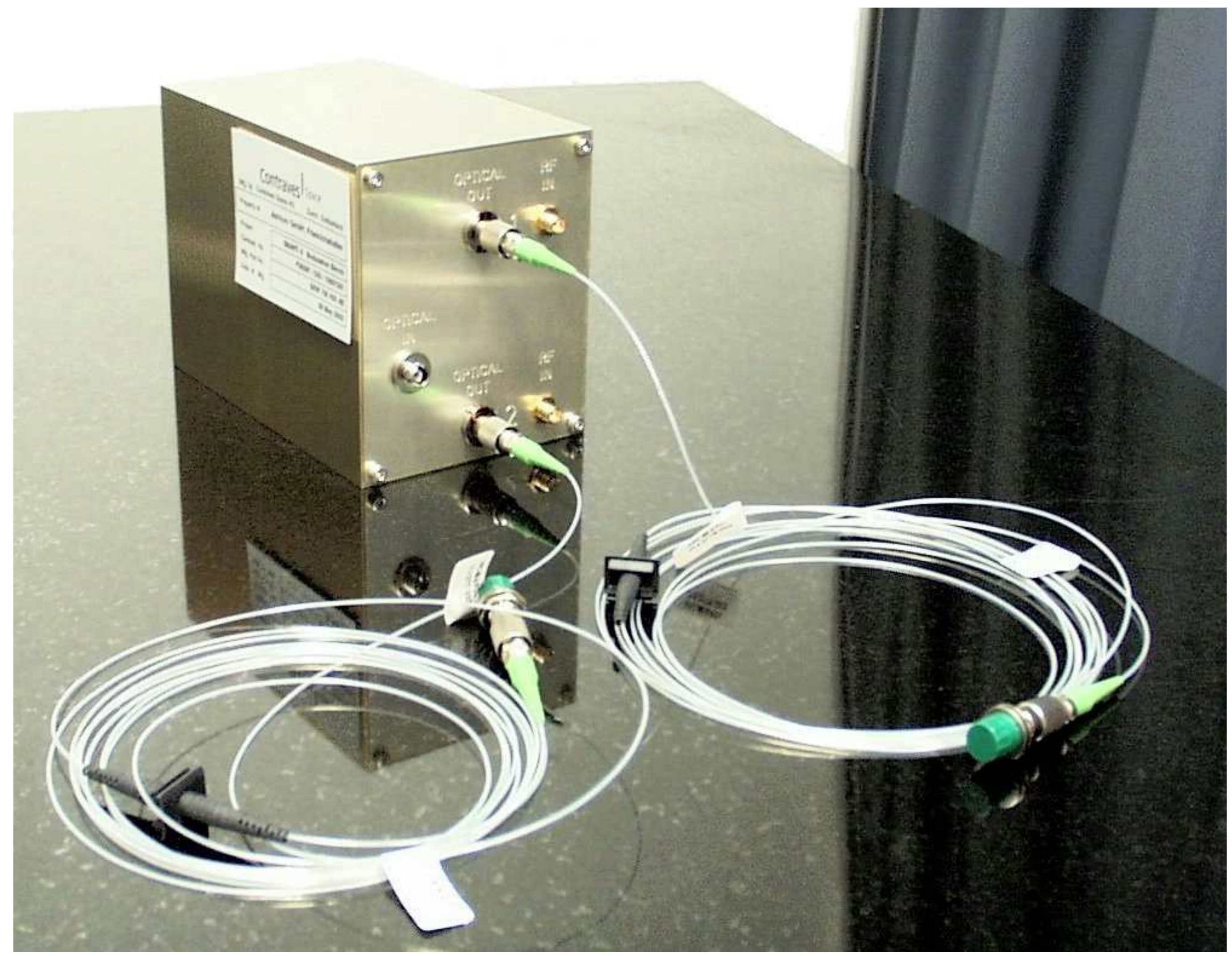

needs further development.

Modulation bench at TNO

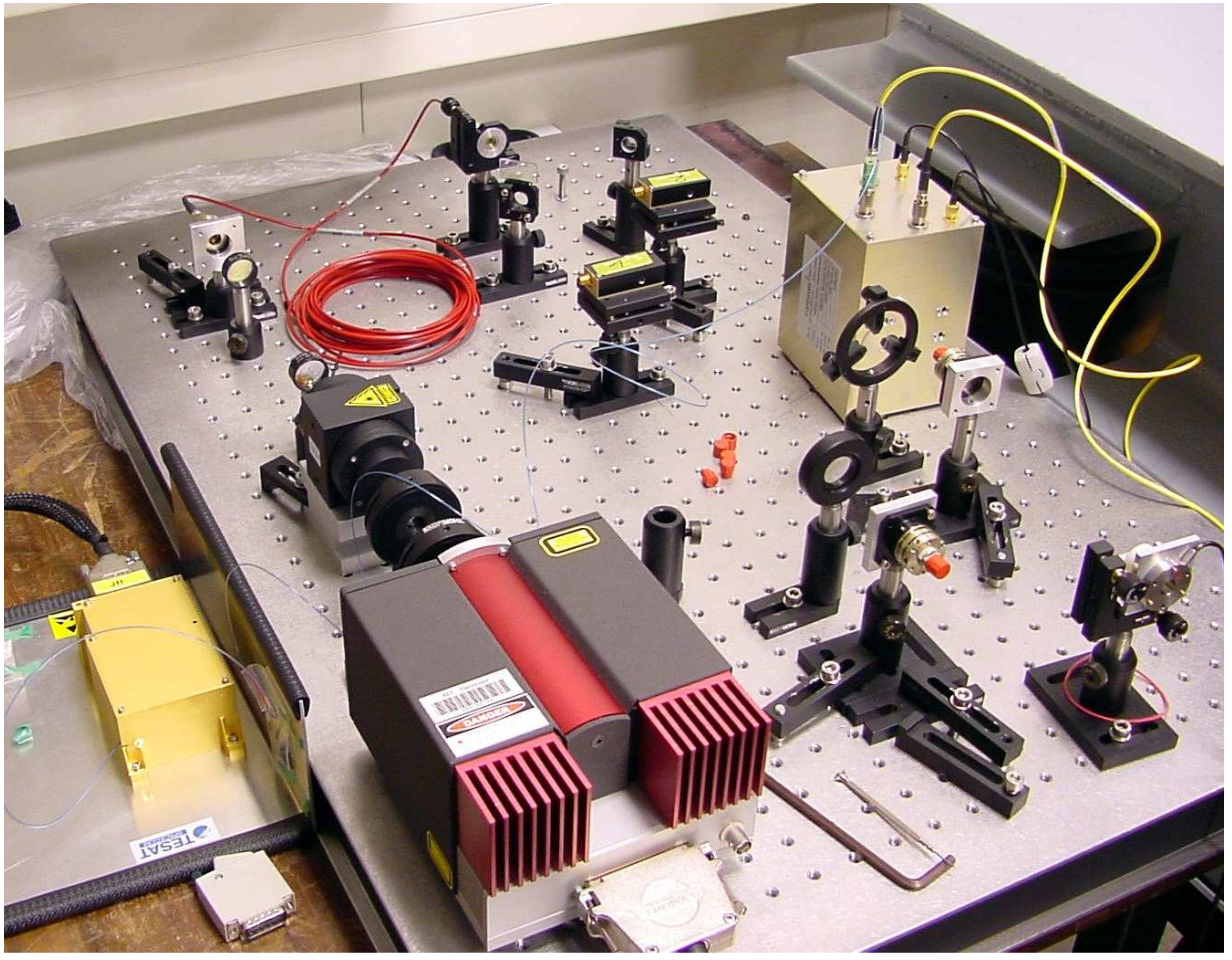

Functional overview

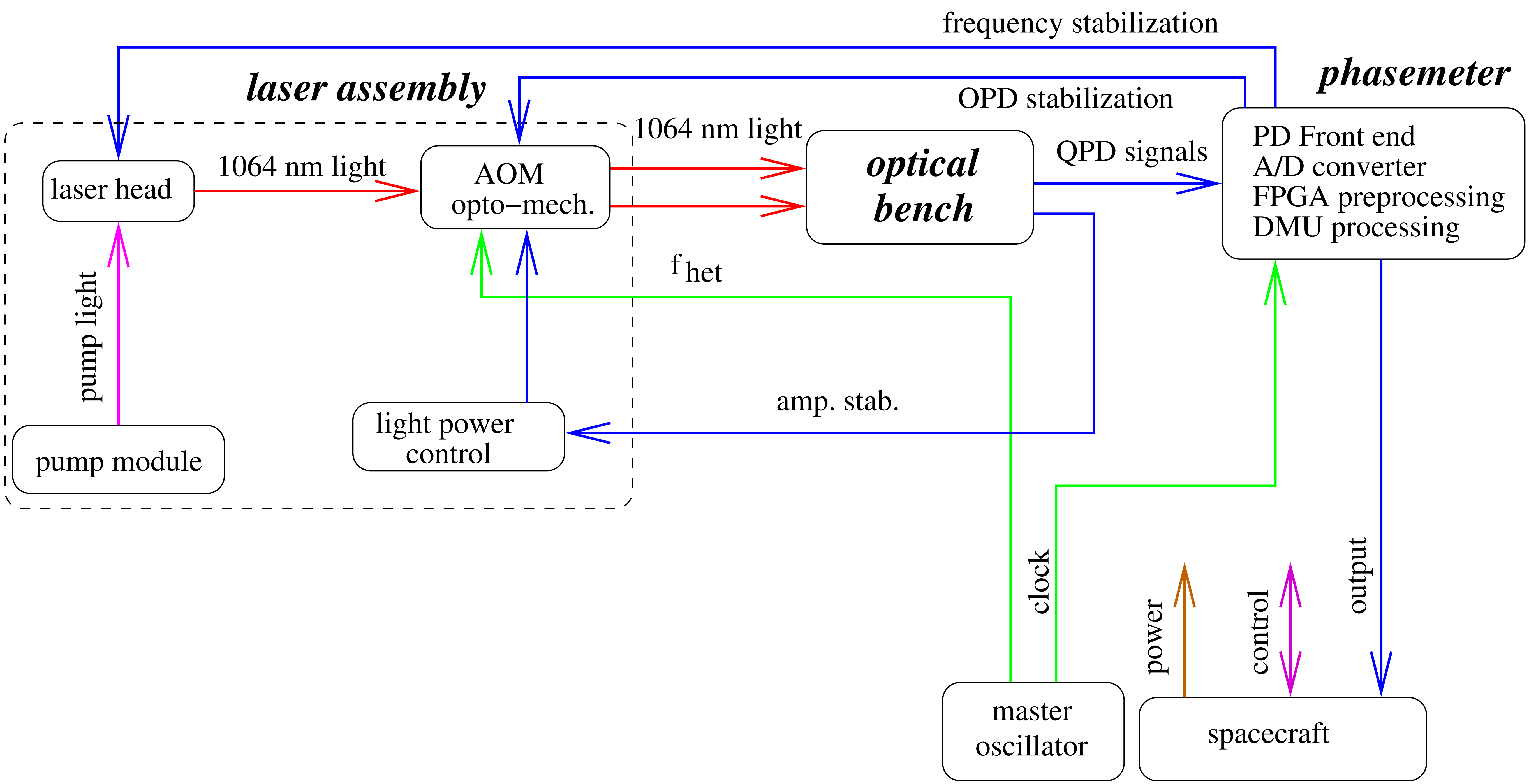

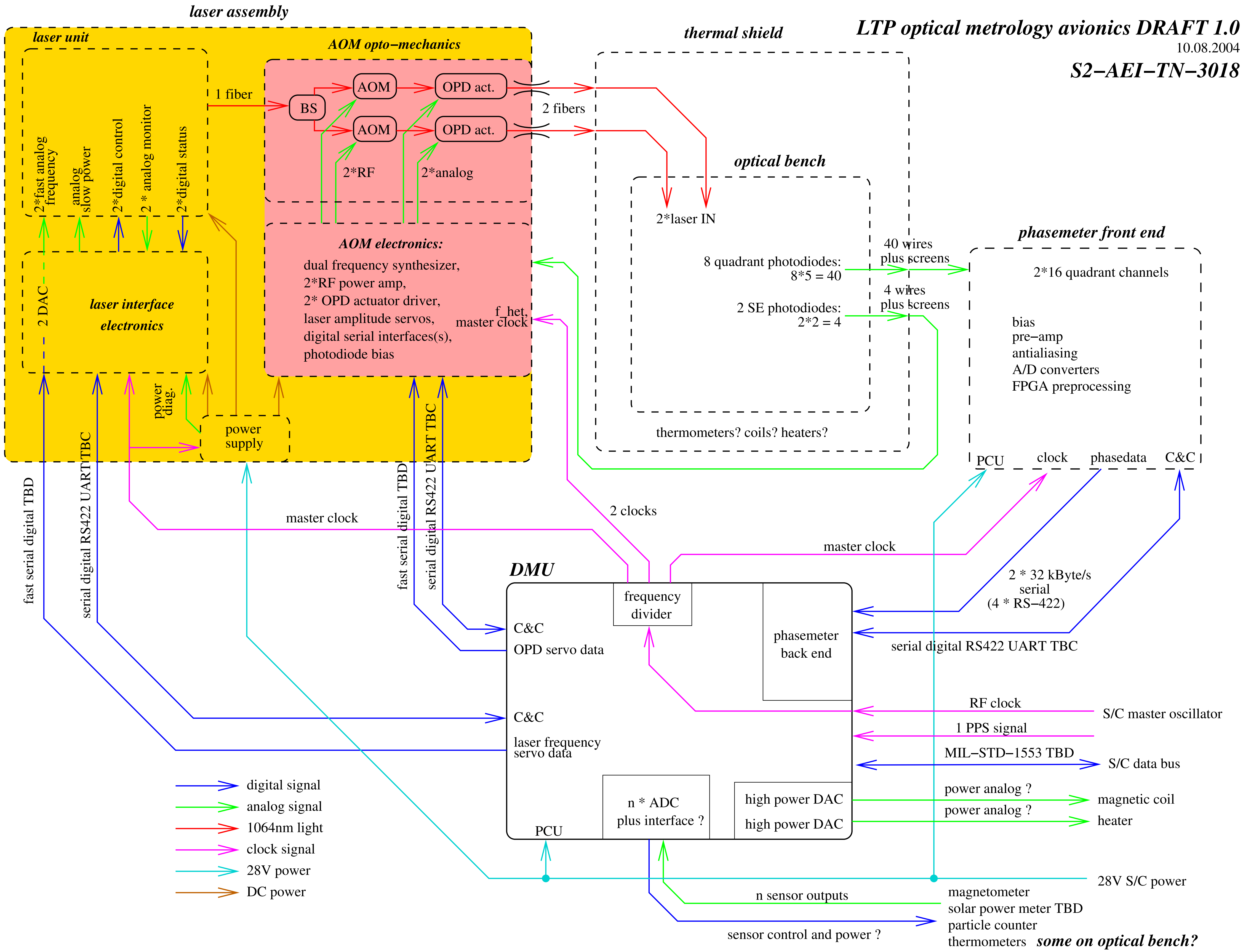
LTP optical metrology avionics DRAFT 1.0
10.08.2004
S2−AEI−TN−3018
laser assembly
laser unit
AOM opto−mechanics
thermal shield
optical bench
phasemeter front end
1 fiber
BS
AOM
AOM
OPD act.
OPD act.
2 fibers
2*RF
2*analog
2*fast analog frequency
analog slow power
2*digital control
2 * analog monitor
2*digital status
2*laser IN
8 quadrant photodiodes: 8*5 = 40
2 SE photodiodes: 2*2 = 4
40 wires plus screens
4 wires plus screens
2*16 quadrant channels
bias
pre−amp
antialiasing
A/D converters
FPGA preprocessing
PCU
clock
phasedata
C&C
2 DAC
laser interface electronics
AOM electronics:
dual frequency synthesizer,
2*RF power amp,
2* OPD actuator driver,
laser amplitude servos,
digital serial interfaces(s),
photodiode bias
f_het, master clock
power diag.
power supply
thermometers? coils? heaters?
fast serial digital TBD
serial digital RS422 UART TBC
fast serial digital TBD
serial digital RS422 UART TBC
master clock
2 clocks
master clock
DMU
frequency divider
phasemeter back end
2 * 32 kByte/s serial (4 * RS−422)
serial digital RS422 UART TBC
C&C
OPD servo data
C&C
laser frequency servo data
RF clock
S/C master oscillator
1 PPS signal
MIL−STD−1553 TBD
S/C data bus
n * ADC plus interface ?
high power DAC
high power DAC
power analog ?
power analog ?
magnetic coil
heater
PCU
28V S/C power
n sensor outputs
sensor control and power ?
magnetometer
solar power meter TBD
particle counter
thermometers
some on optical bench?
digital signal
analog signal
1064nm light
clock signal
28V power
DC power

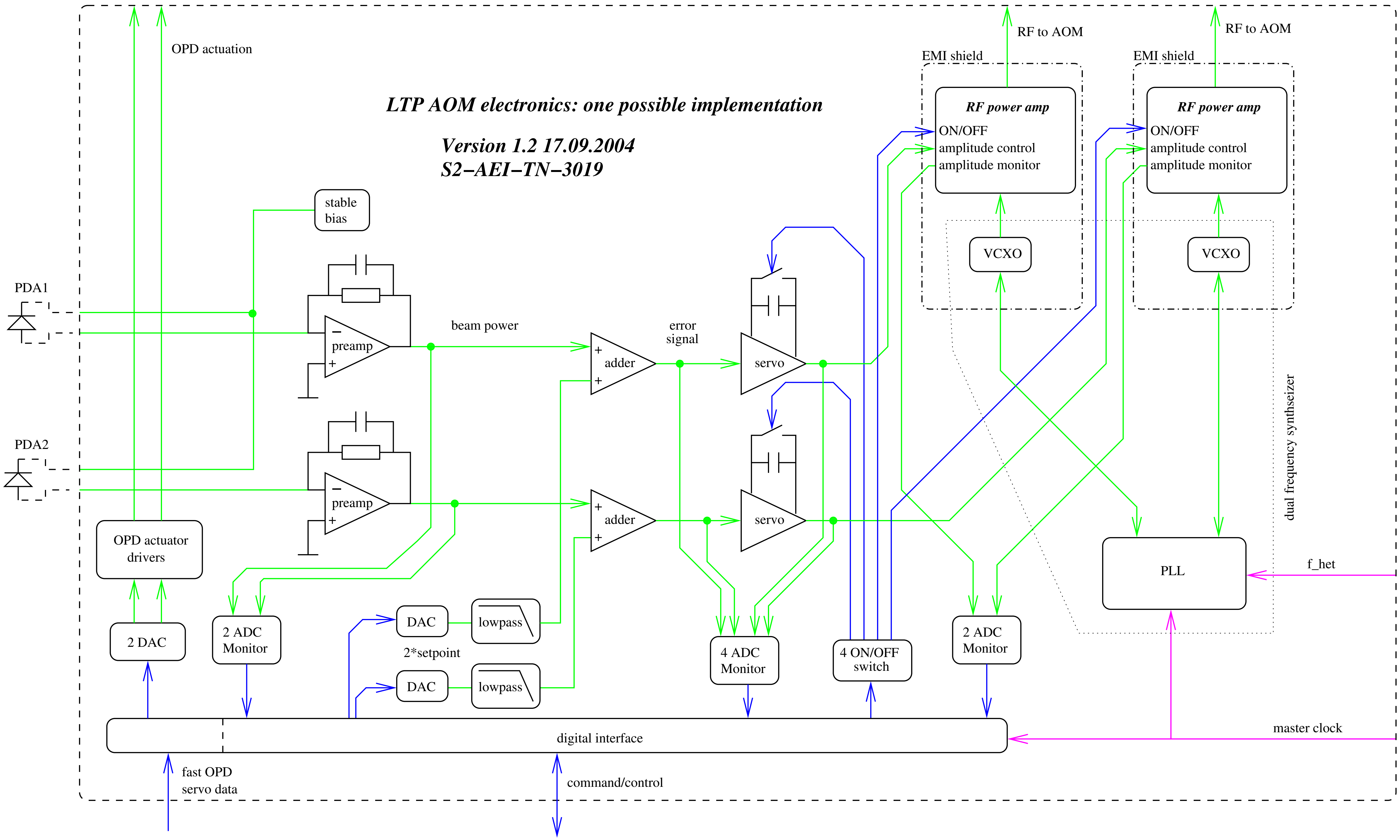

LTP AOM electronics: one possible implementation
Version 1.2 17.09.2004
S2–AEI–TN–3019
OPD actuation
RF to AOM
RF to AOM
EMI shield
EMI shield
RF power amp
ON/OFF
amplitude control
amplitude monitor
RF power amp
ON/OFF
amplitude control
amplitude monitor
VCXO
VCXO
stable
bias
PDA1
PDA2
preamp
preamp
beam power
adder
adder
error
signal
servo
servo
dual frequency synthseizer
PLL
f_het
OPD actuator
drivers
2 DAC
2 ADC
Monitor
DAC
lowpass
2*setpoint
DAC
lowpass
4 ADC
Monitor
4 ON/OFF
switch
2 ADC
Monitor
digital interface
master clock
fast OPD
servo data
command/control

Laser power stabilization

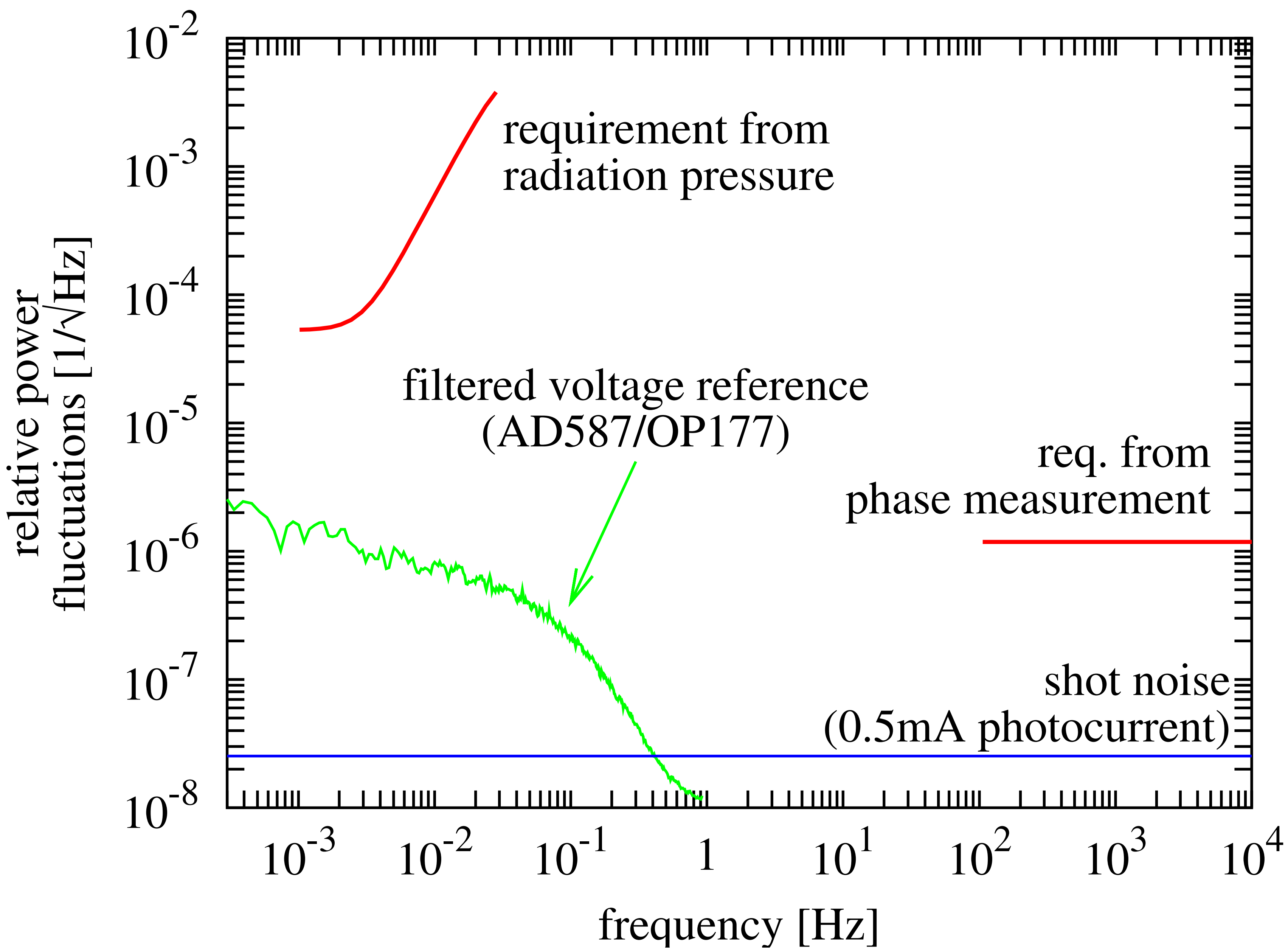

radiation pressure:

$$\frac{\widetilde{\delta P}}{P} < \frac{m\,c\,\omega^2}{2P}\,\widetilde{\delta y} \quad \text{at 1 mHz}$$

phase measurement:

$$\frac{\widetilde{\delta P}}{P} < \frac{c}{2\sqrt{2}}\,\widetilde{\delta \varphi} \quad \text{at } f_{\text{het}}$$

Stabilization via split feedback to Laser pump module (common mode) and AOM RF power (differential mode, BW>50 kHz).

AOM driver

A laboratory prototype of the AOM driver was built and characterized. It consists of two independent TCVCXO's, which are frequency-locked by a PLL to give a constant difference frequency (e.g. 1.6 kHz).

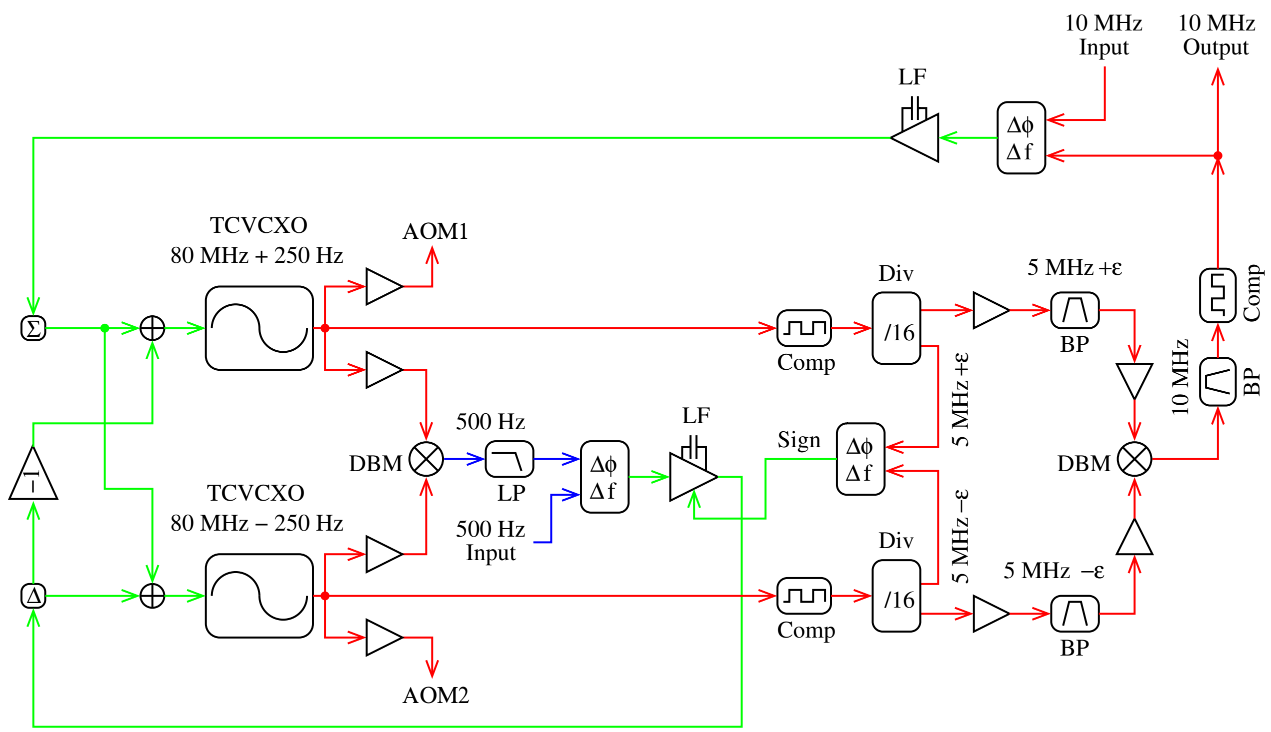

TCVCXO = temperature compensated voltage controlled crystal oscillator
LP = lowpass filter
BP = bandpass filter
LF = loop filter
Comp = comparator to generate logic level signals
Div = digital frequency divider
DBM = double balanced mixer
ΔϕΔf = digital phase/frequency detector

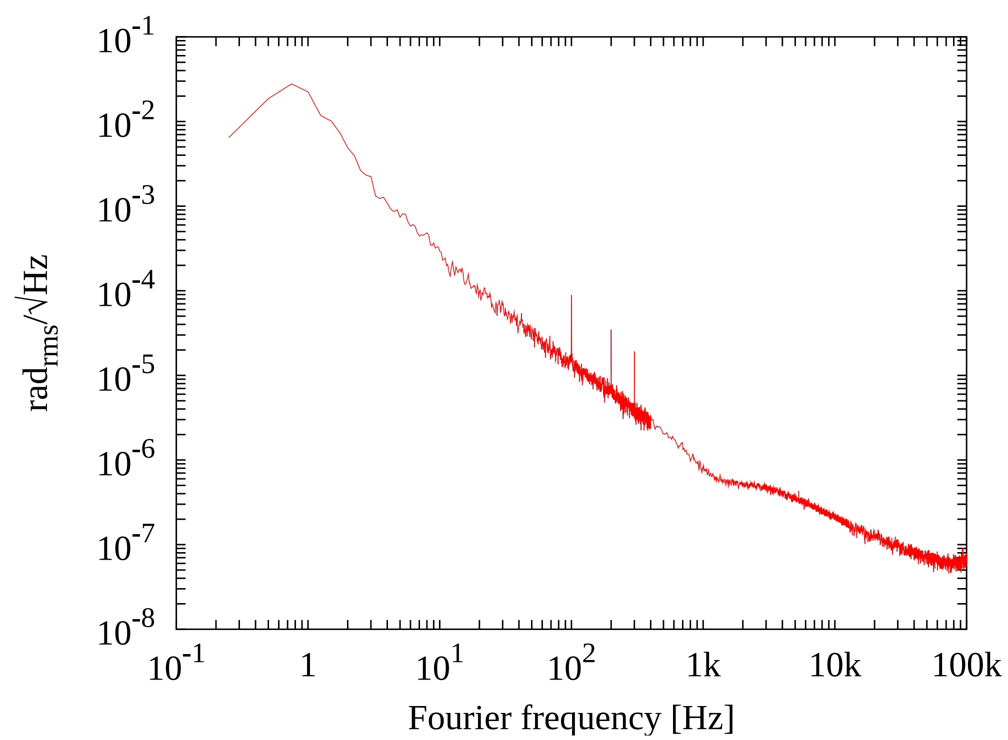

Both the difference frequency ($\approx$ 1.6 kHz) and the average frequency (80 MHz) are controlled by phase-locked loops (PLL).

The phase noise of each oscillator is $< 10^{-6}\,\mathrm{rad}/\sqrt{\mathrm{Hz}}$ at 1 kHz.

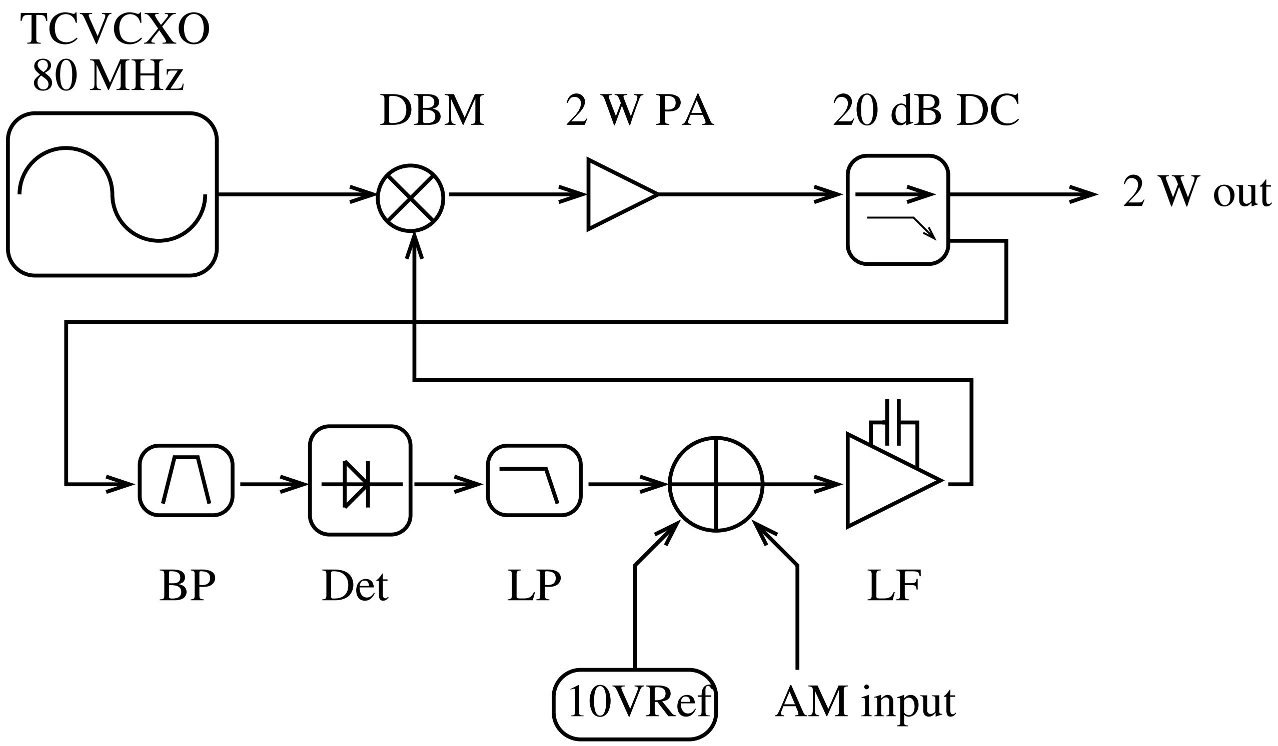

TCVCXO = Temp. compens. VCXO
DBM = double balanced mixer (used as attenuator)
PA = Power Amplifier
DC = Directional Coupler
BP = 80 MHz Bandpass
Det = Schottky Detector
LP = 10 MHz Lowpass
LF = Loop Filter

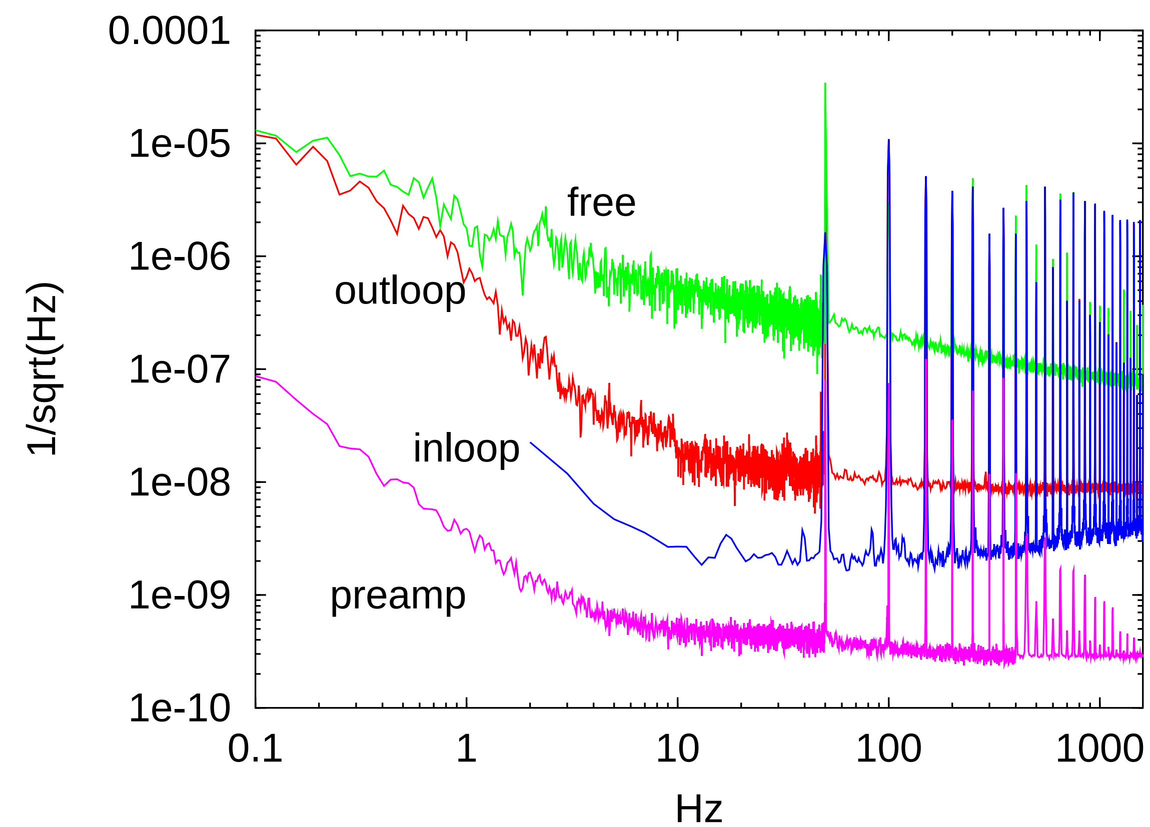

The RF amplitude of each oscillator is stabilized to $\approx 10^{-8}/\sqrt{\mathrm{Hz}}$ at 1 kHz and has a fast input (BW $>$ 100 kHz) to compensate light power fluctuations that are measured at the fiber end.

Laser Frequency noise

Laser frequency fluctuations $\delta\nu = \delta\omega/(2\,\pi)$ cause spurious phase fluctuations $\delta\varphi$ via a **pathlength difference** Δl between the arms.

Conversion factor $\delta\omega$ [rad/s] $\longrightarrow \delta\varphi$:
$\tau = \Delta l/c$, the differential time delay.

Budget: $\delta\varphi < 6\,\mu\text{rad}/\sqrt{\text{Hz}}$
between 3 mHz and 30 mHz

Frequency stability requirement:

$$\widetilde{\delta\nu} = \frac{c}{2\pi\,\Delta l}\,\widetilde{\delta\varphi} = 28\,\frac{\text{kHz}}{\sqrt{\text{Hz}}}\Big/\left[\frac{\Delta l}{1\,\text{cm}}\right]$$

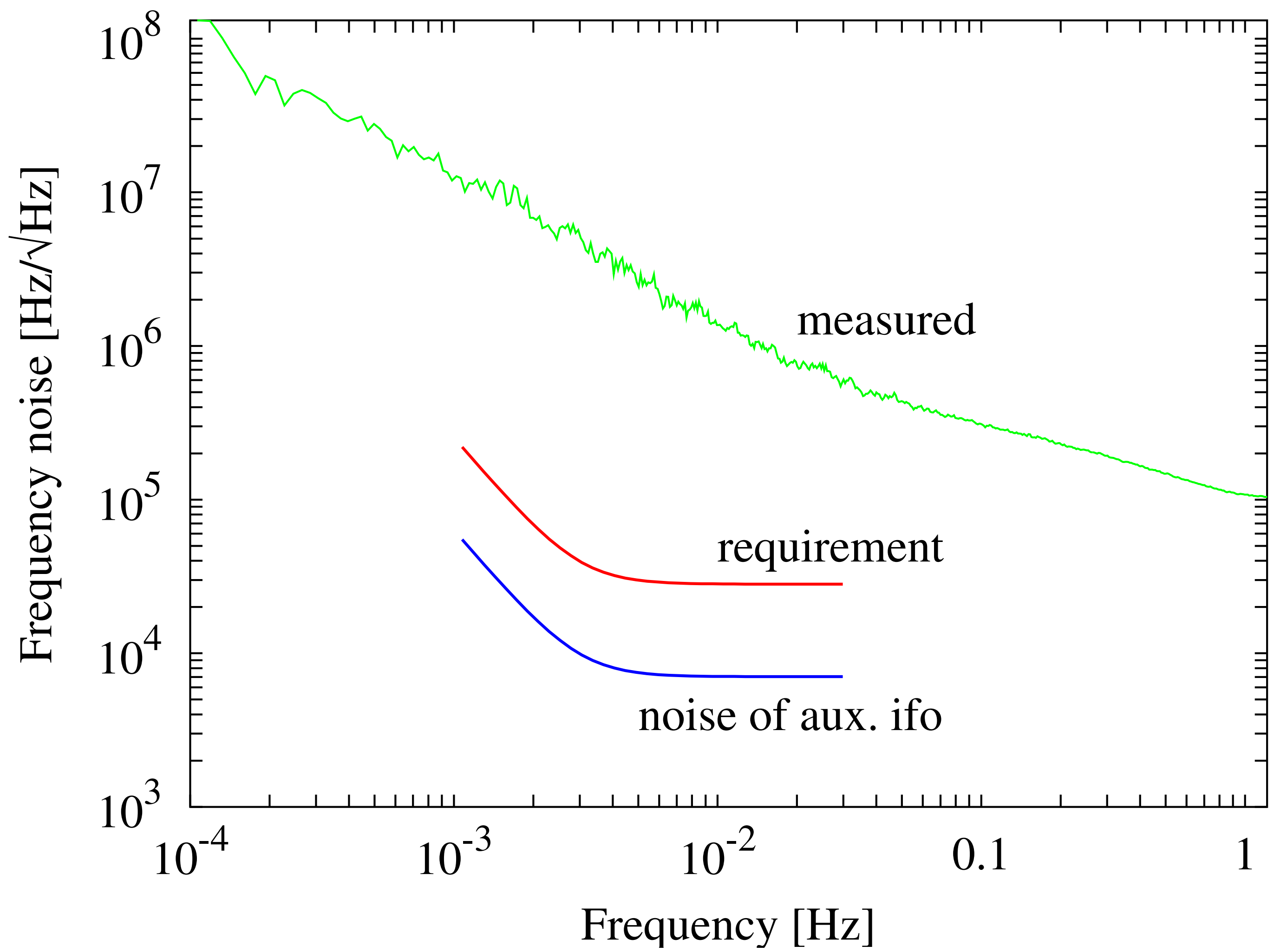

Frequency stabilization

We use the extra interferometer with $\Delta L = 38\,\text{cm}$ as sensor with sufficiently low noise. Two options are:

- Use that signal in a **feedback loop to actively stabilize** the laser **(the baseline)**:

  Required loop gain : ≈ 100 at $30\,\text{mHz}$.

  With a $1/f$ simple integrator as loop filter we need unity gain frequency $> 3\,\text{Hz}$.

  Allowing an extra phase delay of 45° in the loop gain at $3\,\text{Hz}$, the permissible processing time delay is $40\,\text{ms}$ (achievable).

  Small complication with DC feedback: laser is forced to follow drifts of auxiliary interferometer (solvable).

- Do not stabilize the laser but use that signal to **correct the main output signals** for the frequency flucuations thus measured **(fallback option)**. The actual pathlength differences Δl must be known to relatively high precision: $\delta l = 0.1\,\text{mm}$ and $\delta L = 4\,\text{mm}$. Manufacturing to such accuracy is difficult, but measurement during operation is possible.

Phasemeter using SBDFT (Single-Bin Discrete Fourier Transform)

Inputs from one quadrant diode: $x_i = U_A(t_i)$, same for $U_B(t), U_C(t), U_D(t)$.
First step: **SBDFT** achieves data reduction by a factor of ≈ 100:

$$\text{DC components:} \quad \mathrm{DC}_A, \mathrm{DC}_B, \mathrm{DC}_C, \mathrm{DC}_D \quad \text{(real)}: \quad \mathrm{DC}_A = \sum_{i=0}^{n-1} x_i,$$

$$f_{\text{het}}\,\text{components:} \quad \mathrm{F}_A, \mathrm{F}_B, \mathrm{F}_C, \mathrm{F}_D: \quad \Re(\mathrm{F}_A) = \sum_{i=0}^{n-1} x_i \cdot c_i, \quad \Im(\mathrm{F}_A) = \sum_{i=0}^{n-1} x_i \cdot s_i.$$

The constants s_i and c_i are pre-computed: $c_i = \cos\left(\frac{2\pi\, i\, k}{n}\right), s_i = \sin\left(\frac{2\pi\, i\, k}{n}\right)$.

At the moment, our prototype uses PC software. Prototypes close to the LTP phasemeter (using FPGAs for this step) are under construction in Hannover and Birmingham:

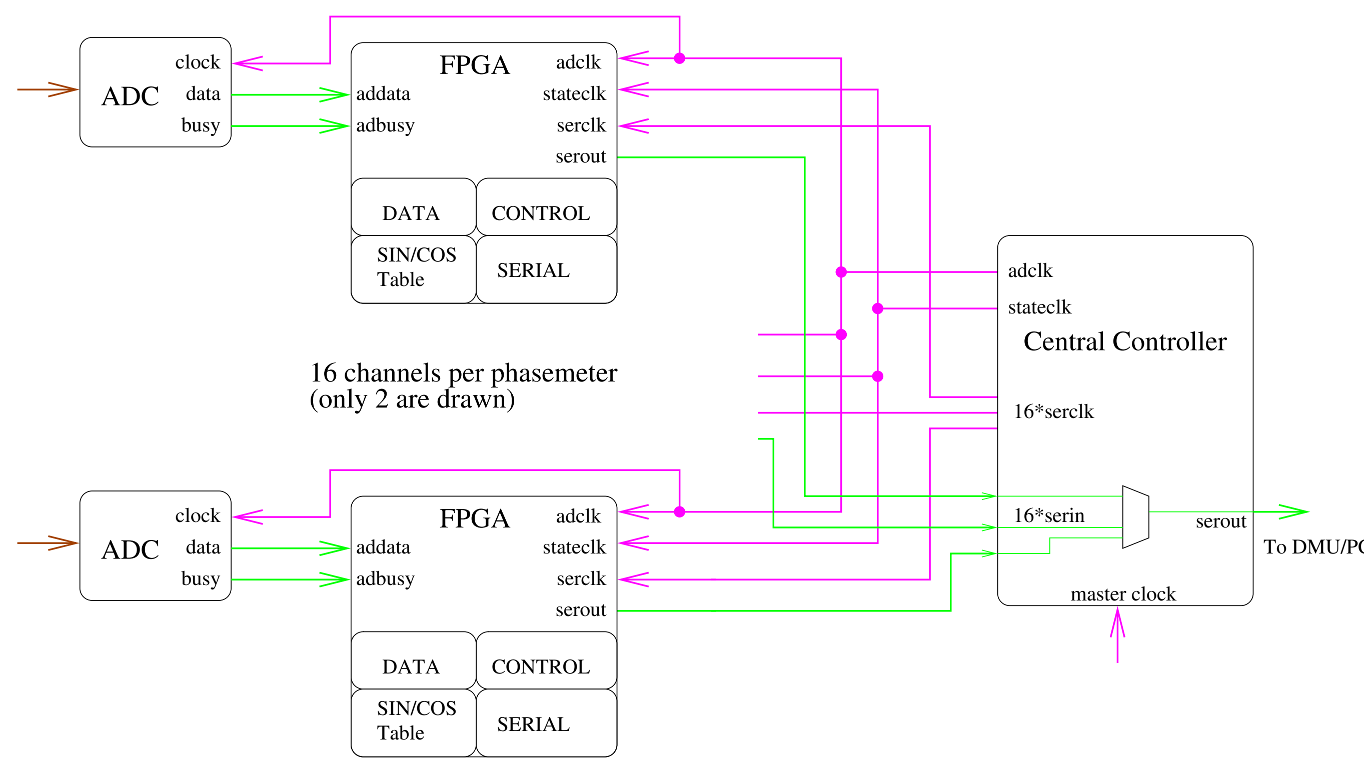

SBDFT phasemeter and Doppler shift*

The SBDFT method requires f_{het} to be exactly centered in on output bin of the DFT. Hence f_{het} and f_{samp} are derived from one common master clock. The expected exact result is:
$\text{DFT}_0 = (-1)^k \, \frac{n}{2} \, e^{\mathrm{i}\,\phi}$, where $n =$ NFFT, $k =$ bin, $\phi =$ true phase.
With a frequency offset δ (expressed in bin widths, typically -0.5. . . 0.5), we get, however:

$$\text{DFT} = (-1)^k \frac{\left(e^{2\,\mathrm{i}\,\delta\,\pi} - 1\right) \left(e^{\mathrm{i}\left(\phi + \frac{4\,(\delta+k)\,\pi}{n}\right)} - \cos(\phi) - \mathrm{i}\left(2\,e^{\frac{2\,\mathrm{i}\,\delta\,\pi}{n}} - 1\right)\sin(\phi)\right)}{2\,e^{\mathrm{i}\,\delta\,\pi}\left(e^{\frac{2\,\mathrm{i}\,\delta\,\pi}{n}} - 1\right)\left(e^{\frac{2\,\mathrm{i}\,(\delta+2\,k)\,\pi}{n}} - 1\right)}$$

- error occurs only during test mass motion and is **non accumulative**.
- not a significant problem for LTP, but possibly important for LISA.
- remedy 1: time-domain window functions (e.g. Hanning, Kaiser-Bessel etc.) effectively remove the error term.
- remedy 2: The error is predictable (depends only on ϕ and δ, which are both measured). It can hence be explicitely corrected.

*'Stopwatch' type phasemeters seem to exhibit a similar phenomenon.

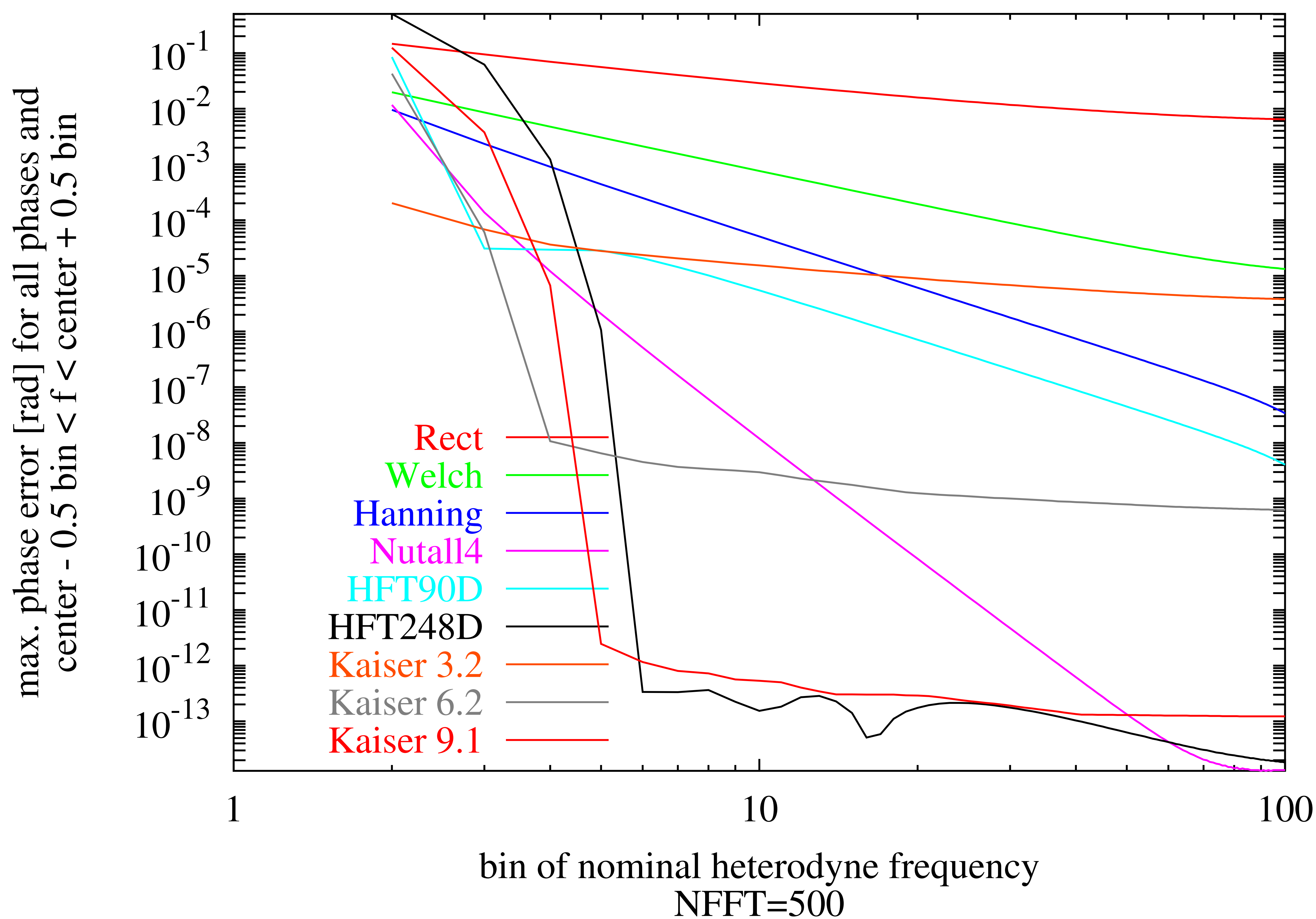
max. phase error [rad] for all phases and
center - 0.5 bin < f < center + 0.5 bin
10^-1
10^-2
10^-3
10^-4
10^-5
10^-6
10^-7
10^-8
10^-9
10^-10
10^-11
10^-12
10^-13
Rect
Welch
Hanning
Nutall4
HFT90D
HFT248D
Kaiser 3.2
Kaiser 6.2
Kaiser 9.1
1
10
100
bin of nominal heterodyne frequency
NFFT=500

An Idea for a LISA phasemeter

The SBDFT phase measurement technique works well and has excellent Signal-to-Noise ratio, if the frequency is within one output bin.

It becomes rather straightforward if the frequency stays nearly centered in the bin.

This might be reached by a digital PLL that generates a local oscillator LO via a numerical controlled oscillator (NCO).

The end result consists of 2 components:
– the LO phase,
– the residual phase measured by the phasemeter.

Most obvious open questions:

– required vs. obtainable PLL loop bandwidth.

– USO Noise propagation.

– interaction with modulation sidebands.

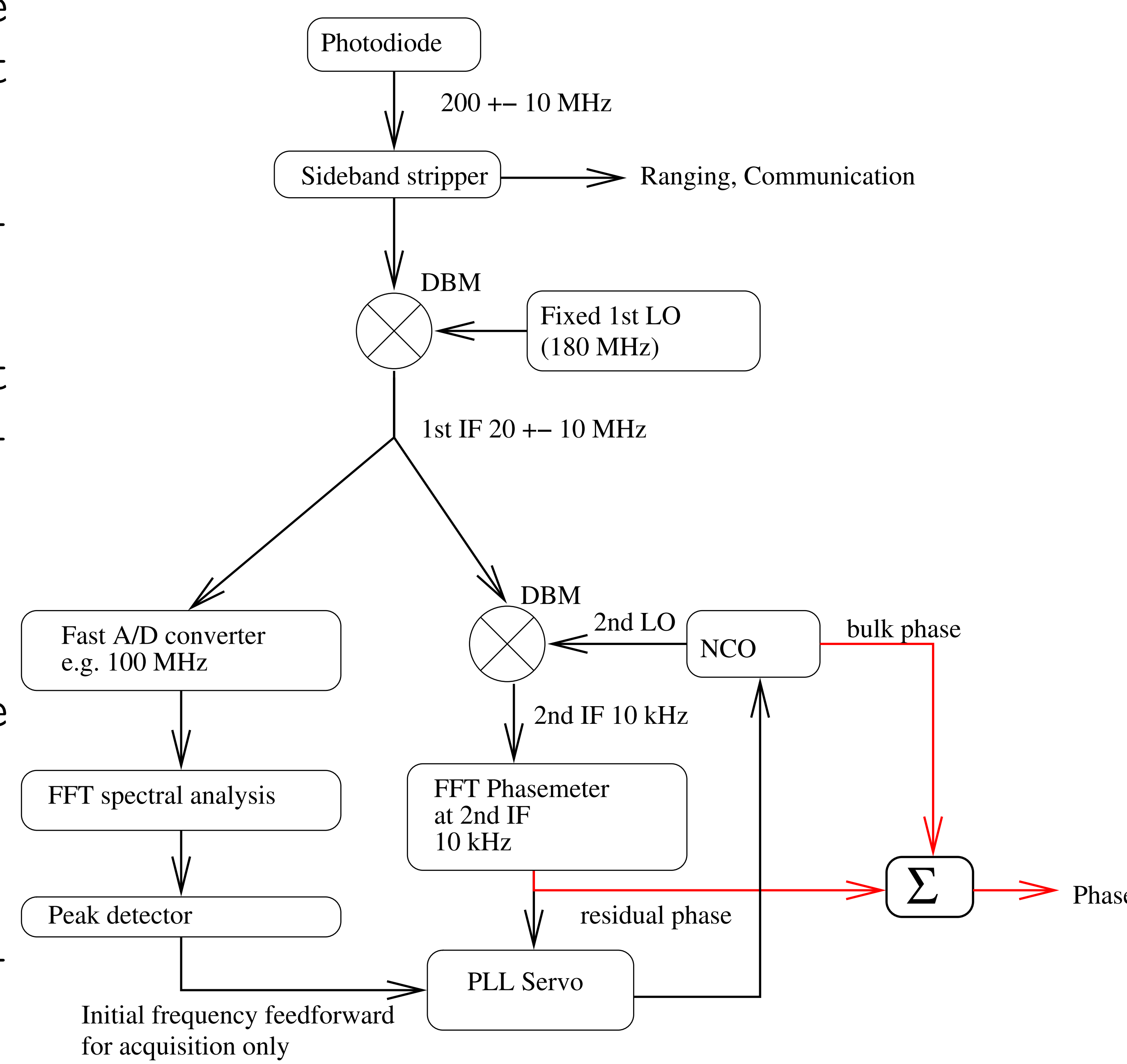

Further processing in DMU

Longitudinal Signal:
$\mathsf{F}_\Sigma^{(1)} = \mathsf{F}_A + \mathsf{F}_B + \mathsf{F}_C + \mathsf{F}_D$ the total f_{het} amplitude on the first quadrant diode, and
$\mathsf{F}_\Sigma^{(2)}$ for the second (reference) quadrant diode equivalently.
$\varphi_{\text{long}} = \arg(\mathsf{F}_\Sigma^{(1)}) - \arg(\mathsf{F}_\Sigma^{(2)}) + n \cdot 2\pi$, (integer n from phasetracking algorithm).

Alignment signals, independently on each diode:
$\mathsf{F}_{\text{Left}} = \mathsf{F}_A + \mathsf{F}_D$: amplitude in left half, $\mathsf{DC}_{\text{Left}} = \mathsf{DC}_A + \mathsf{DC}_D$: average in left half,
$\mathsf{F}_{\text{Right}}$, $\mathsf{F}_{\text{Upper}}$, $\mathsf{F}_{\text{Lower}}$, $\mathsf{DC}_{\text{Right}}$, $\mathsf{DC}_{\text{Upper}}$, $\mathsf{DC}_{\text{Lower}}$ equivalently.

The DC (center of gravity) signals:

$$\Delta x = \frac{\mathsf{DC}_{\text{Left}} - \mathsf{DC}_{\text{Right}}}{\mathsf{DC}_\Sigma}, \quad \Delta y = \frac{\mathsf{DC}_{\text{Upper}} - \mathsf{DC}_{\text{Lower}}}{\mathsf{DC}_\Sigma},$$

The DWS (differential wavefront sensing) signals:

$$\Phi_x = \arg\left(\frac{\mathsf{F}_{\text{Left}}}{\mathsf{F}_{\text{Right}}}\right), \quad \Phi_y = \arg\left(\frac{\mathsf{F}_{\text{Upper}}}{\mathsf{F}_{\text{Lower}}}\right),$$

Alignment signals are obtained from each quadrant diode individually (no reference needed)
$\longrightarrow$ Rejection of several common mode noise sources.

Optical windows

There will be 4 transmissions through an optical window of approx. 5 mm thickness in the main $x_1 - x_2$ measurement path:

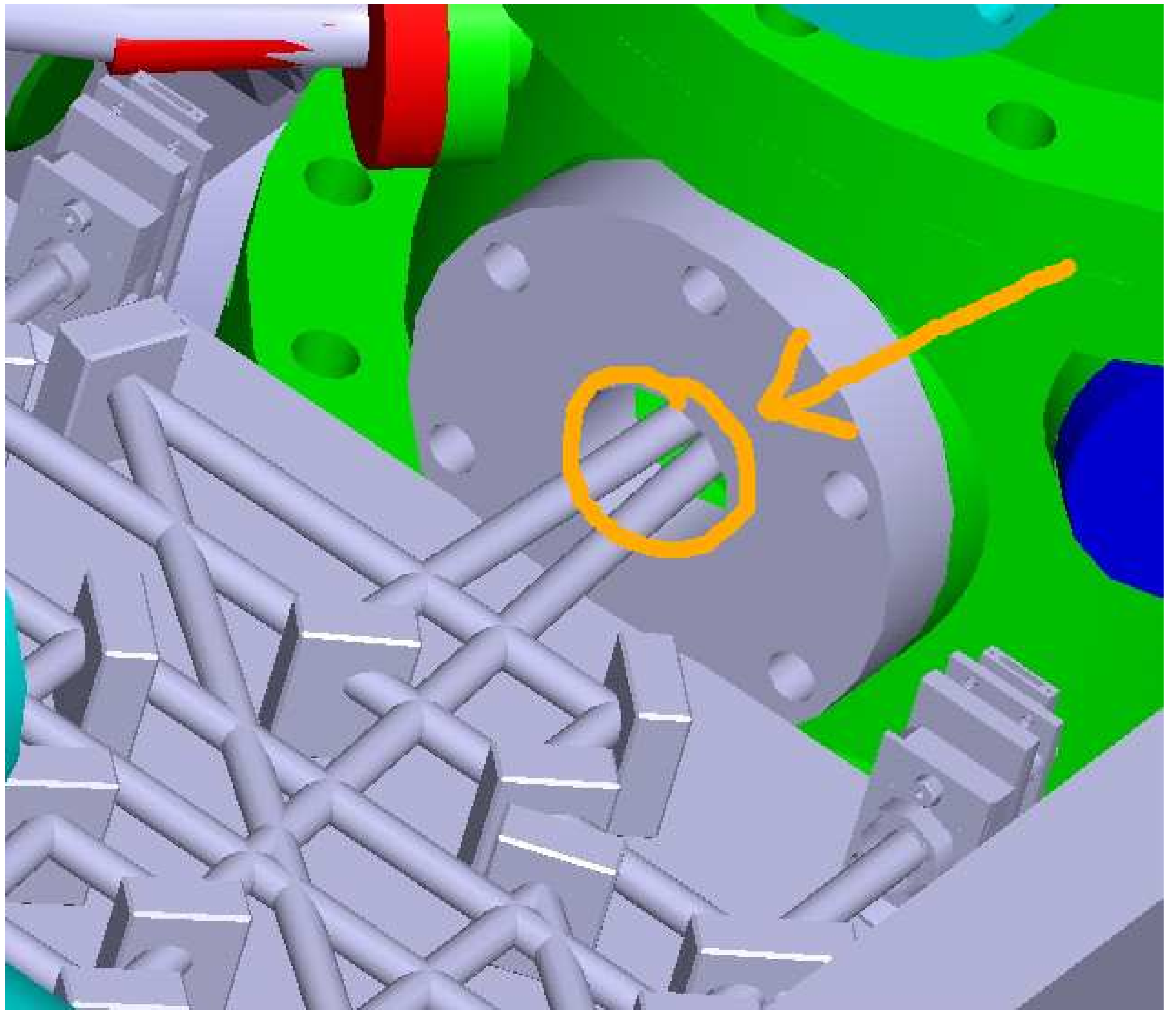

Pathlength effects

Four major disturbing effects on the optical pathlength are expected:

Thermal variation of optical pathlength.

Stress-induced change in refractive index.

mechanical motion of the window in z-direction.

mechanical tilt fluctuations of the window.

The sum of all noise contributions of one window (in double pass) is counted as one interferometer noise source and allocated a bufget of $1\,\mathrm{pm}/\sqrt{\mathrm{Hz}}$. Hence the window effects contribute no more than $1\,\mathrm{pm}/\sqrt{\mathrm{Hz}}$ in the x_1 measurement and no more than $2\,\mathrm{pm}/\sqrt{\mathrm{Hz}}$ in the $x_1 - x_2$ measurement. Each effect is allocated $0.33\,\mathrm{pm}/\sqrt{\mathrm{Hz}}$ (for one window double pass).

Thermal variation of optical pathlength:

$\Delta s = \Delta T \times L \times \left(\frac{\mathrm{d}n}{\mathrm{d}T} + (n-1)\alpha\right)$.

$\mathrm{d}n/\mathrm{d}T + (n-1)\alpha$ is $\approx 5\,\mathrm{ppm/K}$ for most glasses (e.g. BK7).

Athermal glasses (e.g. Ohara S-PHM52, Schott N-FK51 and Schott N-FK56) have <u>0.5 ... 1 ppm/K</u>.

The Schott glasses have a high $\alpha \approx$ 15ppm/K, not well matched to Ti.

The best candidate that we identifed so far is <u>Ohara S-PHM52</u>.

At 1064 nm, $\mathrm{d}n/\mathrm{d}T + (n-1)\alpha = 0.59\,\mathrm{ppm/K}$.

The linear thermal expansion coefficient α is 10.1 ppm/K, well matched to Ti.

All these athermal glasses are difficult to polish and very **brittle**, which may limit the mounting options. With <u>glueing</u>, care must be taken to avoid high static stresses that might cause the glass to break in thermal cycling.

From $\widetilde{\delta T} = \frac{\widetilde{\delta s}}{L \times \left(\frac{\mathrm{d}n}{\mathrm{d}T} + (n-1)\alpha\right)}$,

a pathlength error of $\widetilde{\delta s} = 0.33\,\mathrm{pm}/\sqrt{\mathrm{Hz}}$

and $L = 12\,\mathrm{mm}$,

the required thermal stability at the window is:

$\widetilde{\delta T} < 4 \cdot 10^{-5}\,\mathrm{K}/\sqrt{\mathrm{Hz}}$

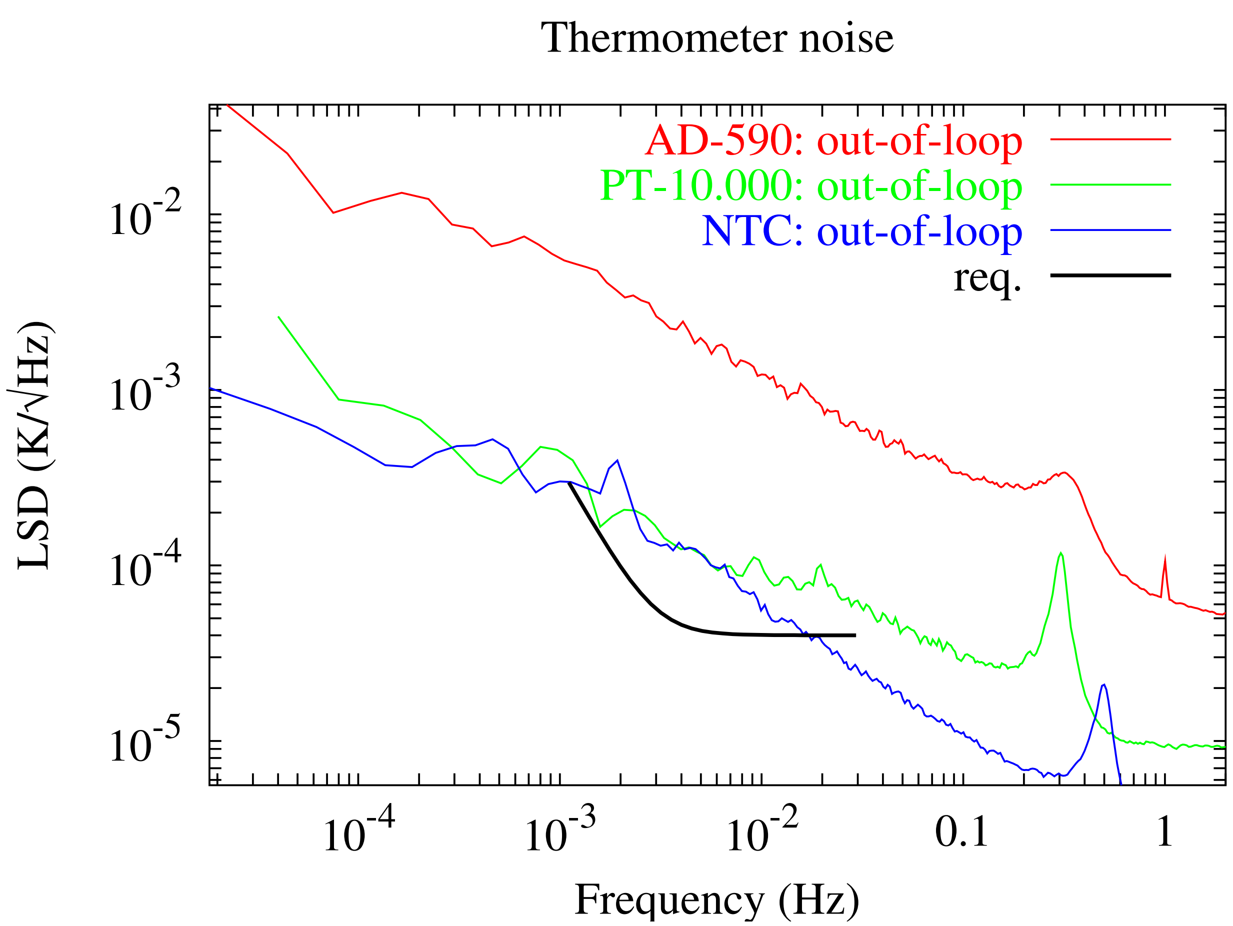

<u>Ohara S-PHM52</u>

Linear thermal expansion $\alpha = 10.1\mathrm{ppm/K}$.

at 1064 nm:

$n = 1.60645$,

$\mathrm{d}n/\mathrm{d}T + (n-1)\alpha = 0.589\,\mathrm{ppm/K}$.

Stress-induced change in refractive index:

While in some materials the stress-induced **birefringence** can be made small, we have here the absolute variation in refractive index, which is never small. The relevant material constant is:

"Photoelastic constant" $\beta = 1.0\,\mathrm{nm/cm}/10^5\mathrm{Pa}$.

For a pathlength error of $0.33\,\mathrm{pm}/\sqrt{\mathrm{Hz}}$ and $L = 12\,\mathrm{mm}$, the required stability of mechanical stress in the window is:

$$\widetilde{\delta\sigma} < 30\,\mathrm{Pa}/\sqrt{\mathrm{Hz}}.$$

We have no knowledge of the real stress fluctuation.
This error might be big.
Mounting of the optical window will be critical (In seal? Au-Sn seal?).
Measuring the thermally induced pathlength fluctuation is essential.

Mechanical motion:

If there is a deviation γ from parallelism and the window moves in z direction by Δz this yields a pathlength error (double-pass):

$$\Delta s = 2\gamma(n-1)\Delta z.$$

For $\gamma = 30''$, $n-1 = 0.6$ and a pathlength error of $0.33\,\mathrm{pm}/\sqrt{\mathrm{Hz}}$ one gets

$$\widetilde{\delta z} < 2\,\mathrm{nm}/\sqrt{\mathrm{Hz}}.$$

If this is difficult, the obvious remedy is to improve the parallelism.

Mechanical tilt fluctuations:

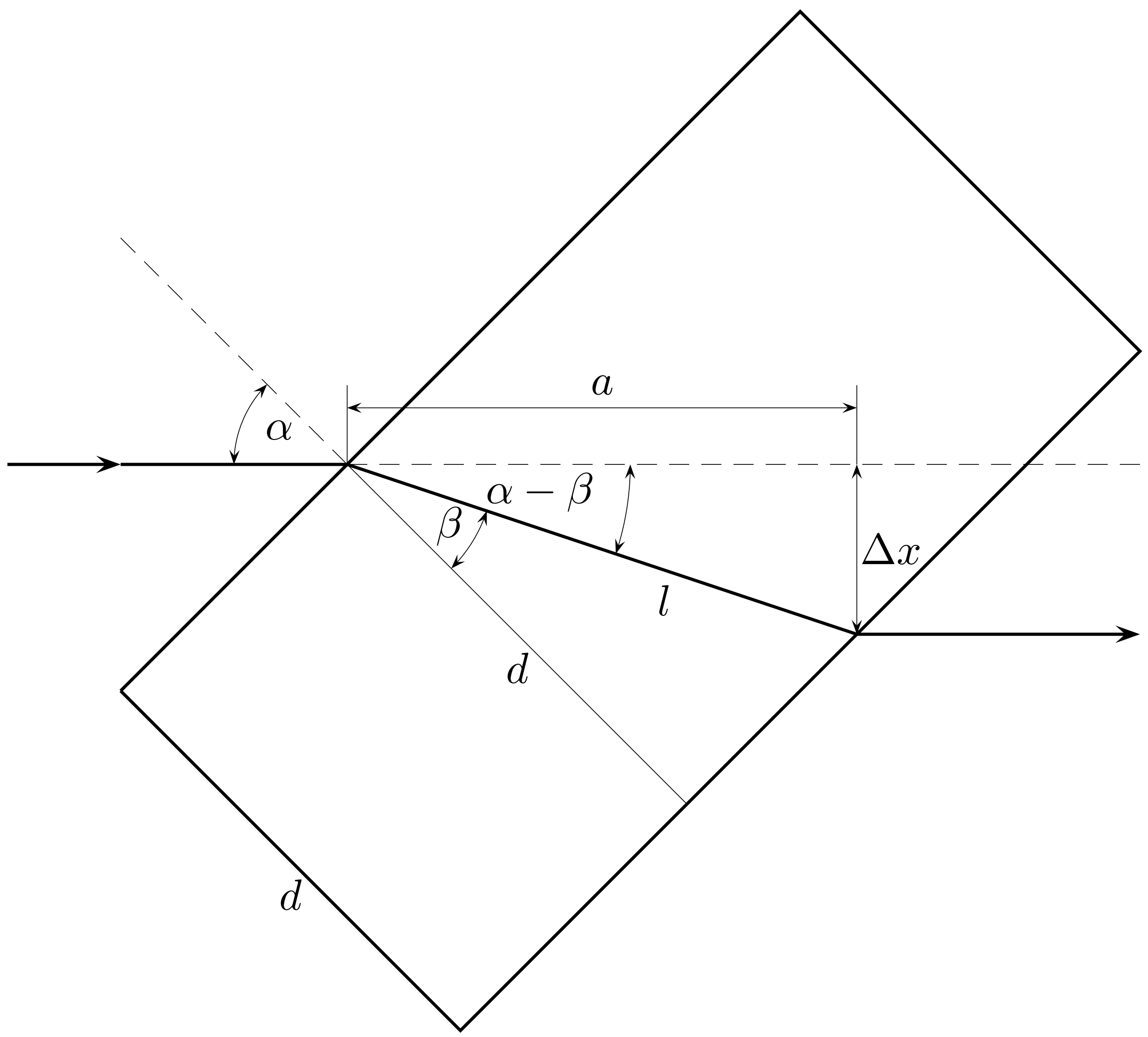

$$l = \frac{d}{\cos\beta}\,,$$

$$a = l\cos(\alpha-\beta),$$

$$\frac{\sin\alpha}{\sin\beta} = n\,,$$

$$\Delta s = nl - a$$

$$\Delta s = d\left(\sqrt{\frac{\cos 2\alpha + 2n^2 - 1}{2}} - \cos\alpha\right)$$

With $\alpha = 2.5^\circ$, $d = 6\,\text{mm}$, $n = 1.6$:

$$\frac{d(\Delta s)}{d\alpha} = 0.98\cdot 10^{-4} \approx 10^{-4}\text{m/rad}$$

For a pathlength error of $0.16\,\text{pm}/\sqrt{\text{Hz}}$ ($0.33\,\text{pm}/2$ because of double-pass) one gets

$$\widetilde{\delta\alpha} < 1.6\,\text{nrad}/\sqrt{\text{Hz}}.$$

If too difficult, α might be reduced at the expense of stray light problems.

Functional, environmental and performance tests

The EM was tested during March and April, 2004 at TNO/TPD, Delft. The tests included:

- Functional tests before and after each other test,
- Thermal vacuum test:
  several cycles 0. . . 40 °C,
- Vibrational test (with dummy masses):
  8 g_{rms} sine and random,
  25 g at the struts.
- Performance tests:
  - Full stroke test: each mirror moved by $\pm 100\,\mu$m,
  - Noise test: mirrors not actuated
  - Tilt test: each mirror tilted by $\pm 1000\,\mu$rad,

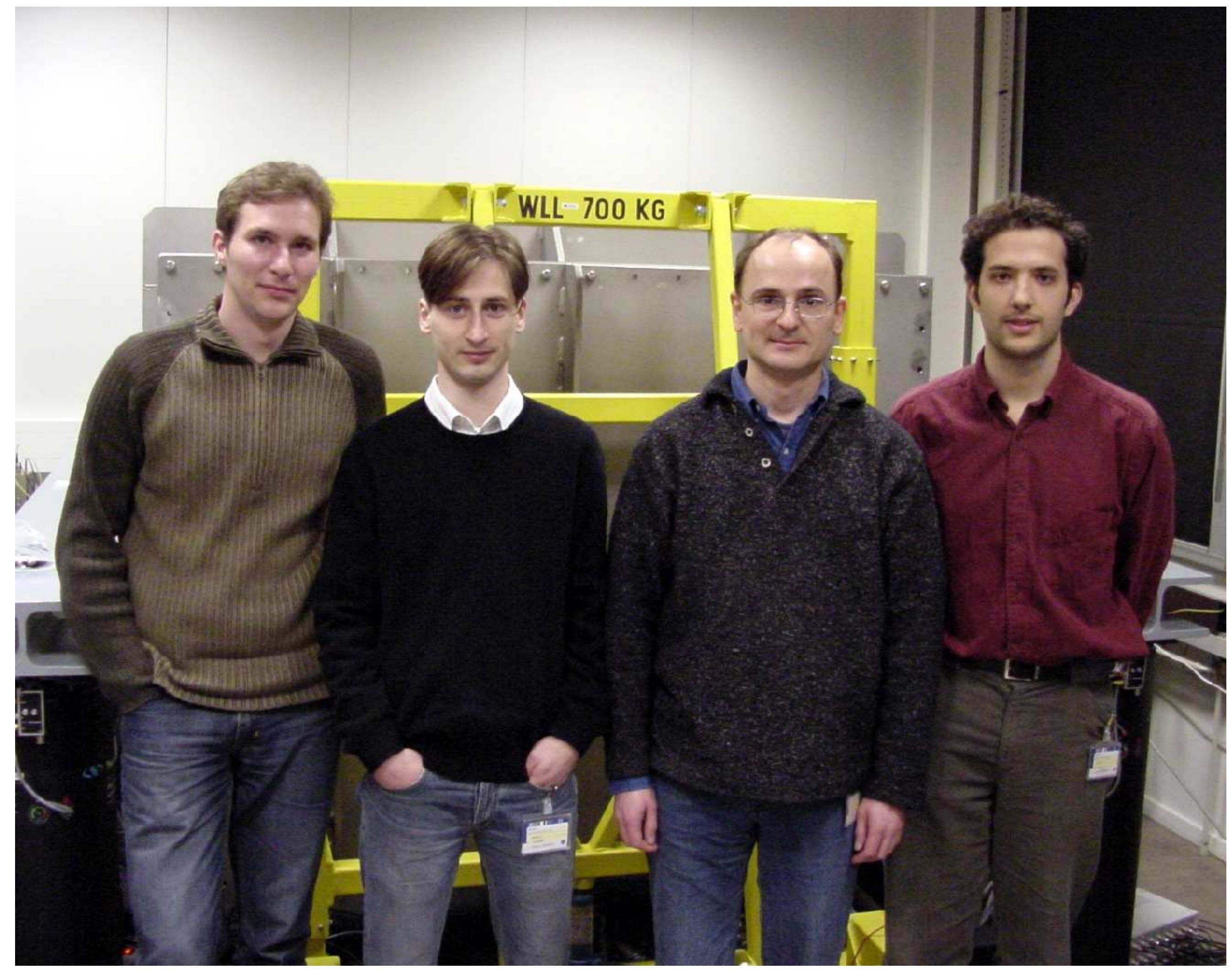

The AEI test team at TNO.

All tests were successful!

EM Test results: high velocity full stroke test (2.9 samples/cycle)

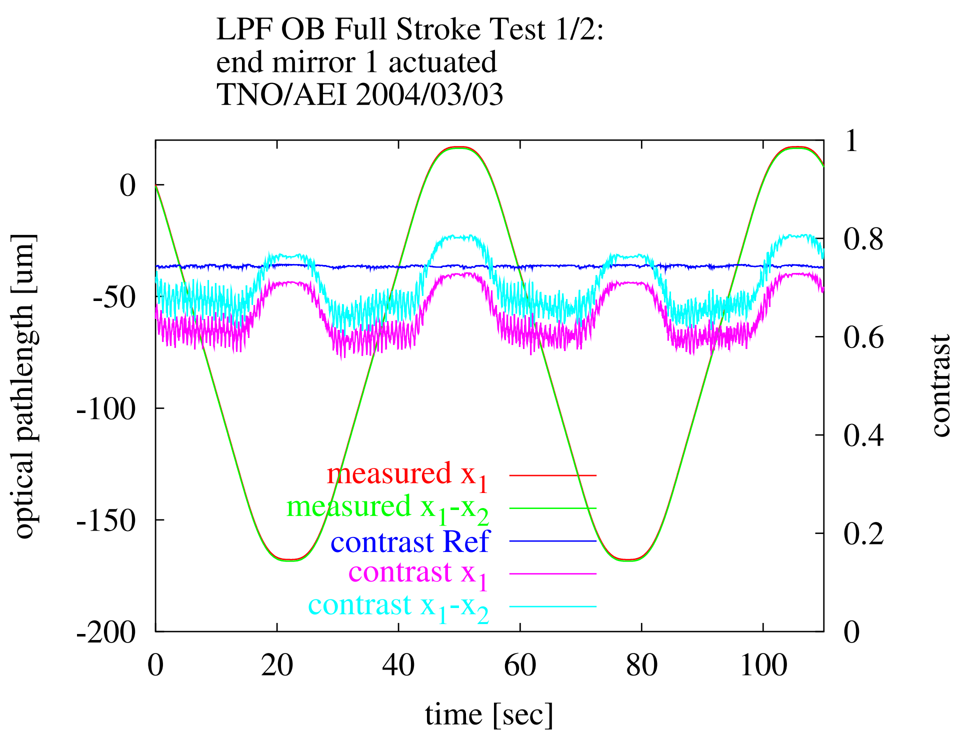

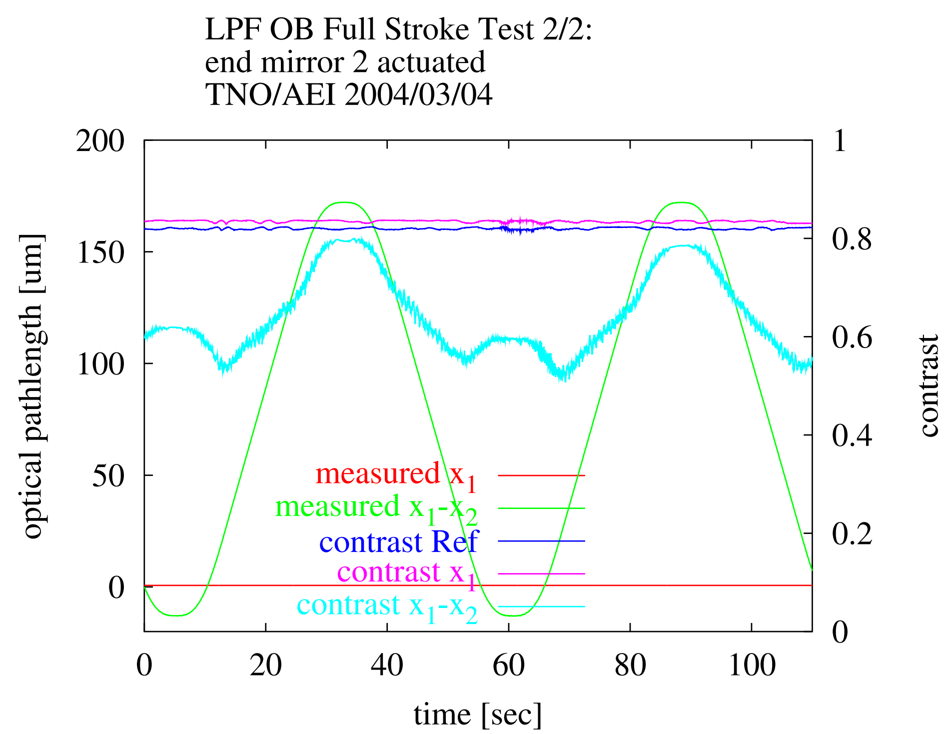

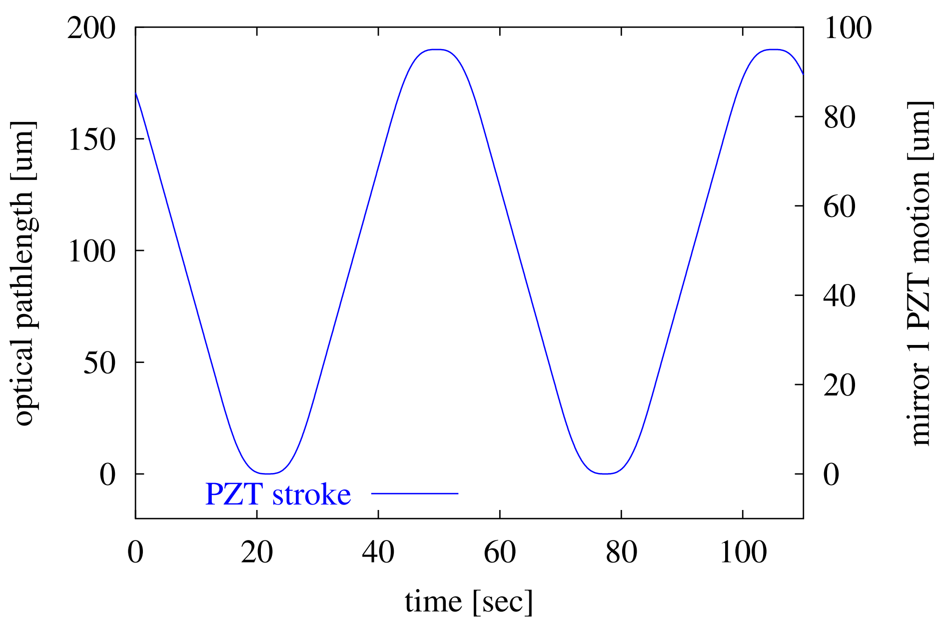

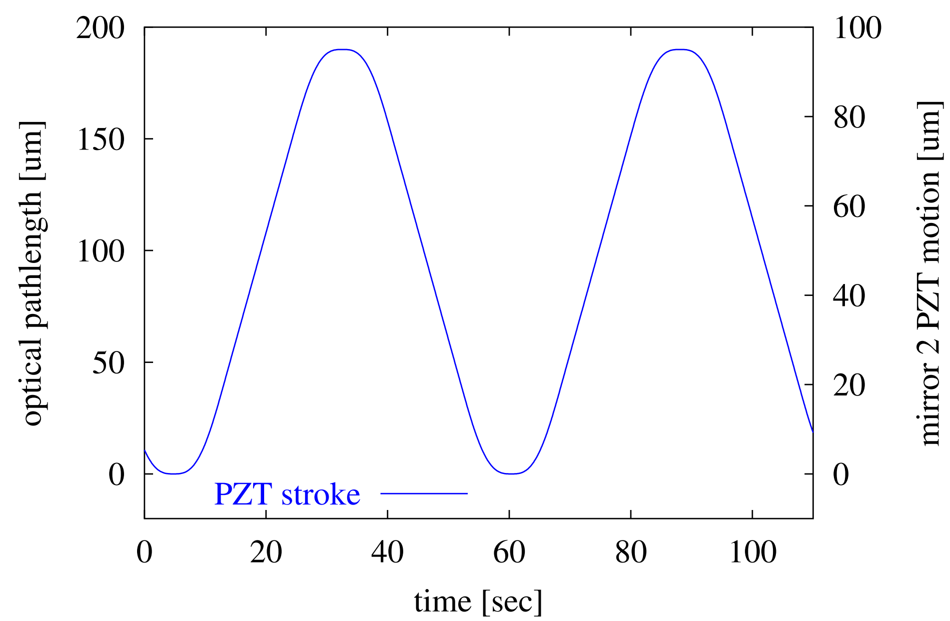

EM Test results: Noise

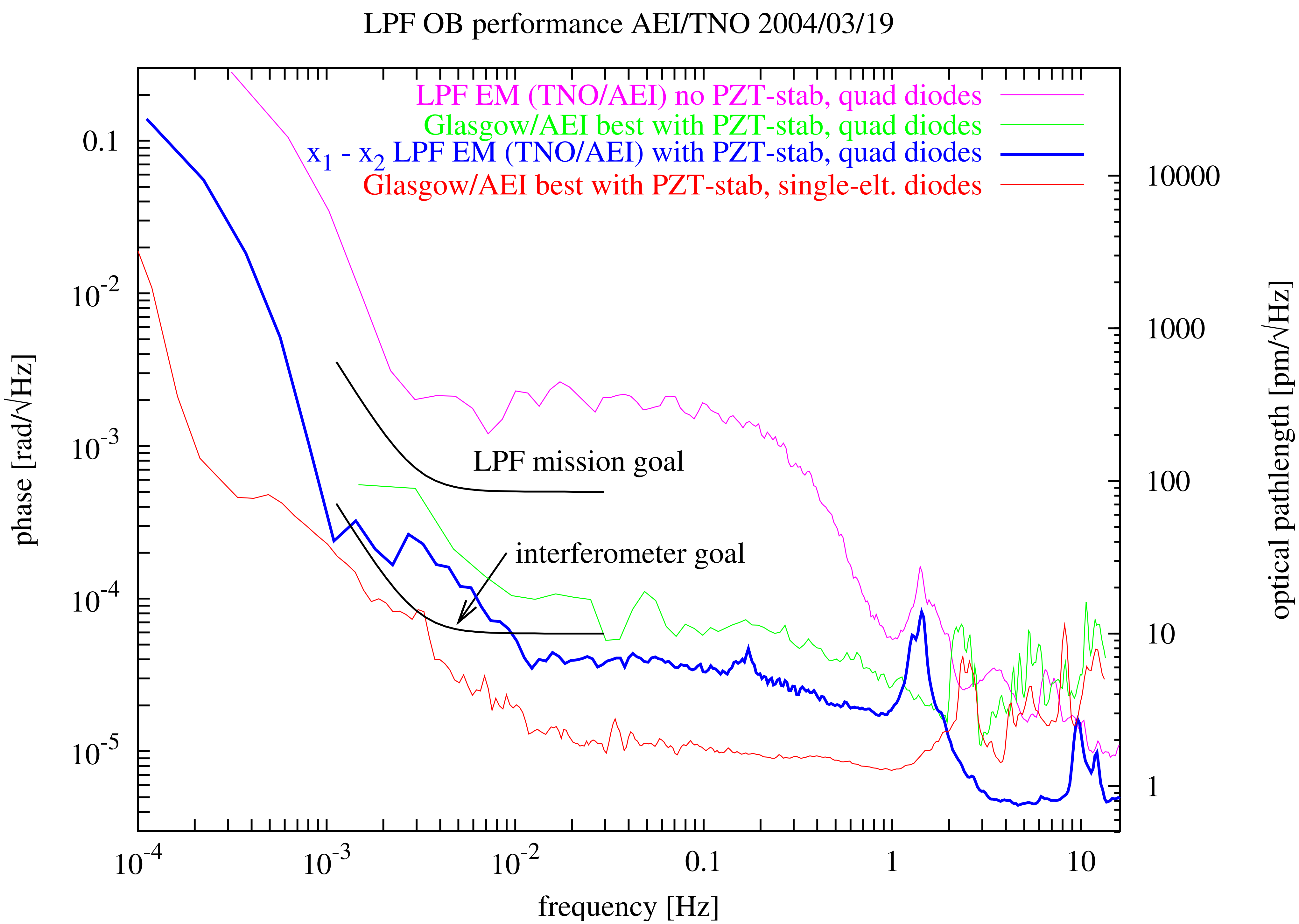

EM Test results: Contrast

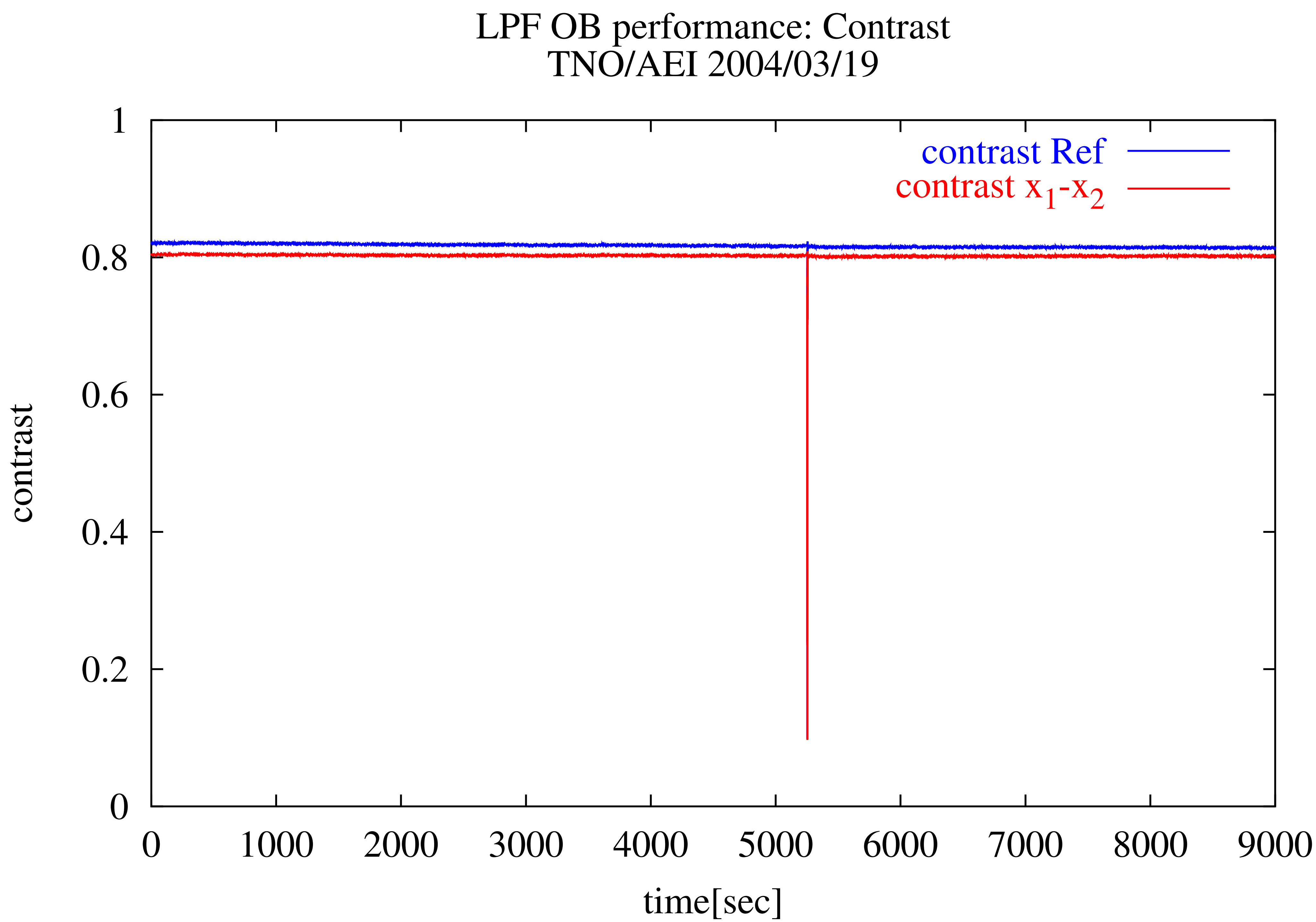

EM Test results: Noise sources 1

At frequencies $< 3\,\mathrm{mHz}$, real motion of the test mirrors is dominant:

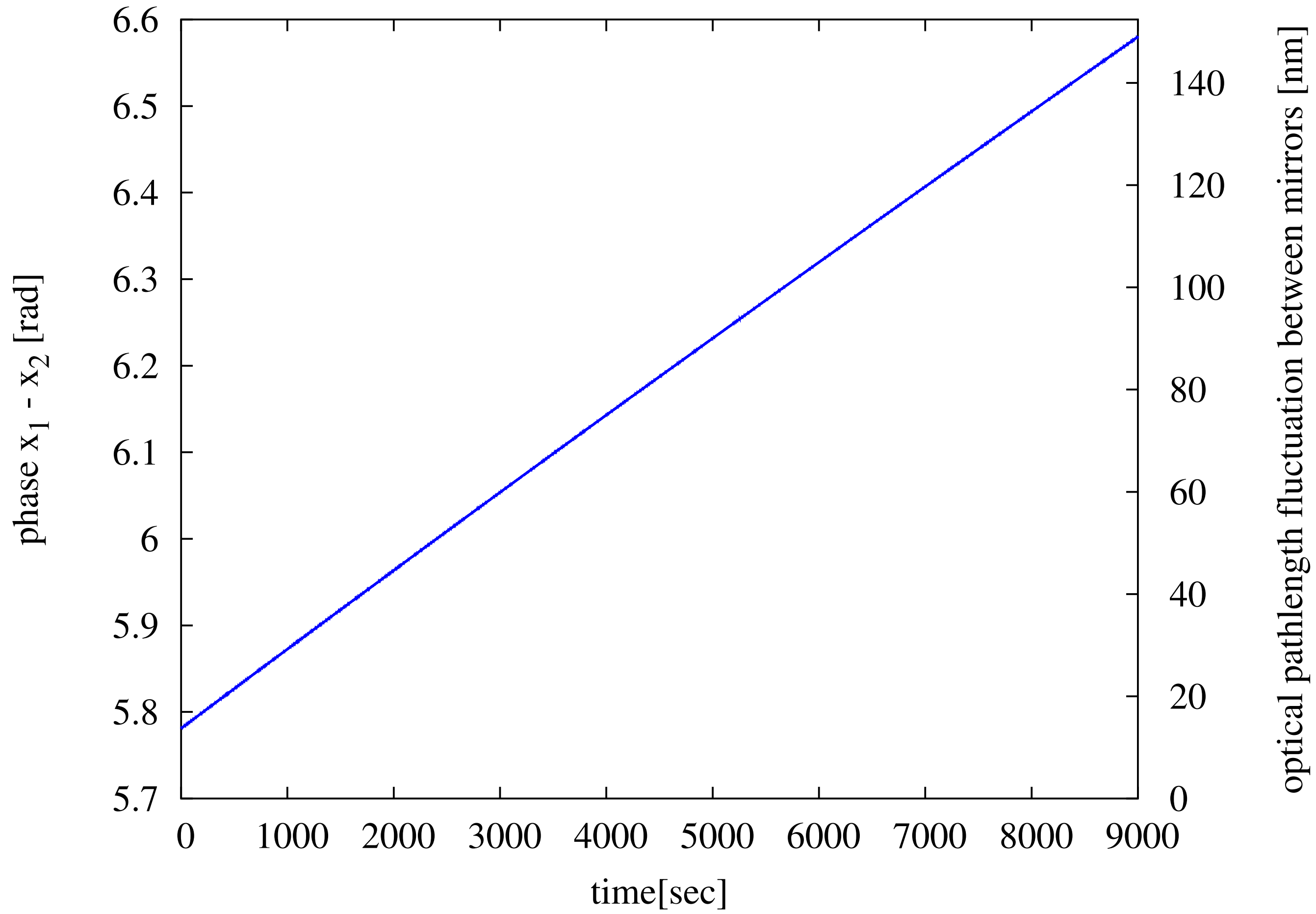

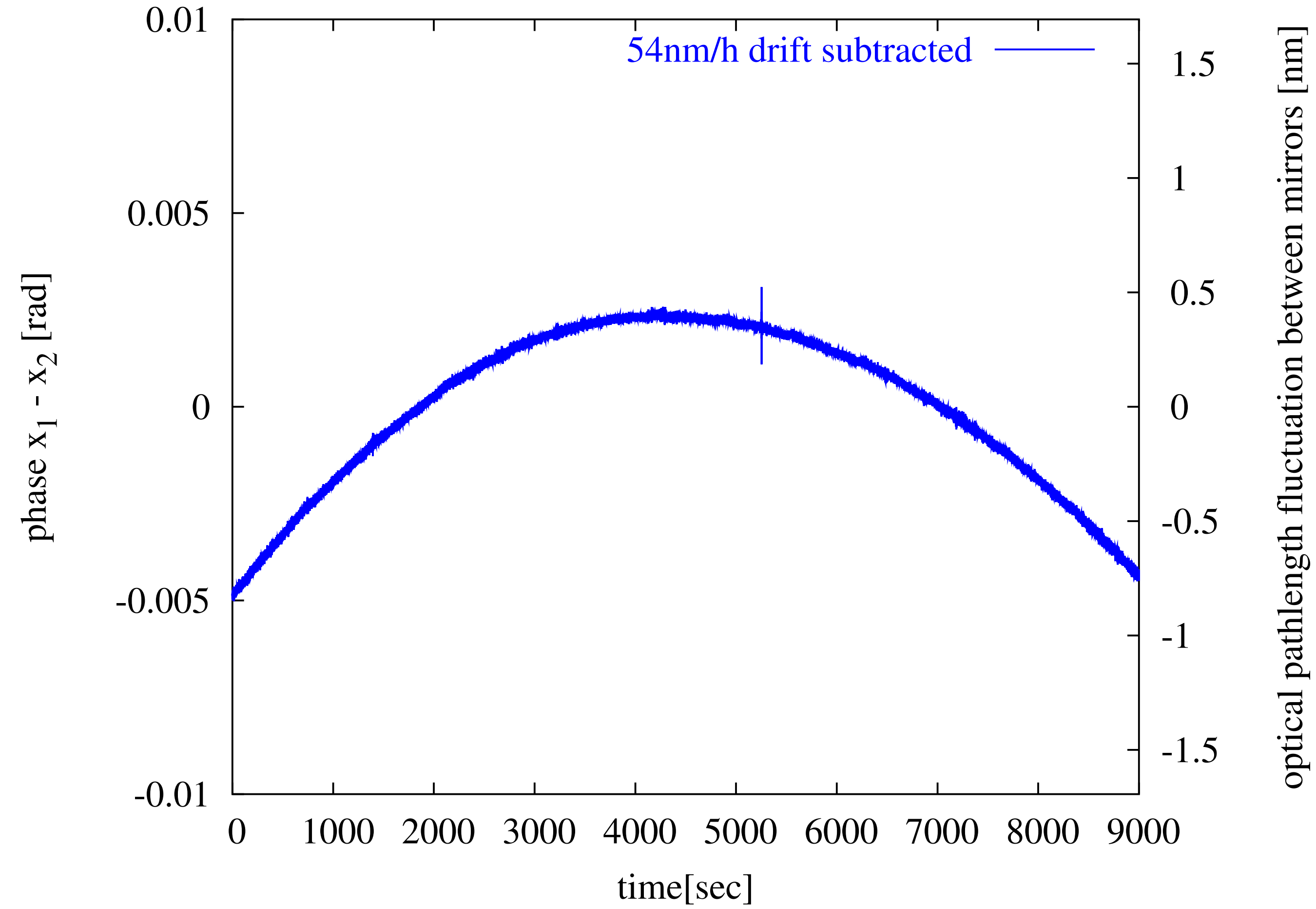

EM Test results: Noise sources 2

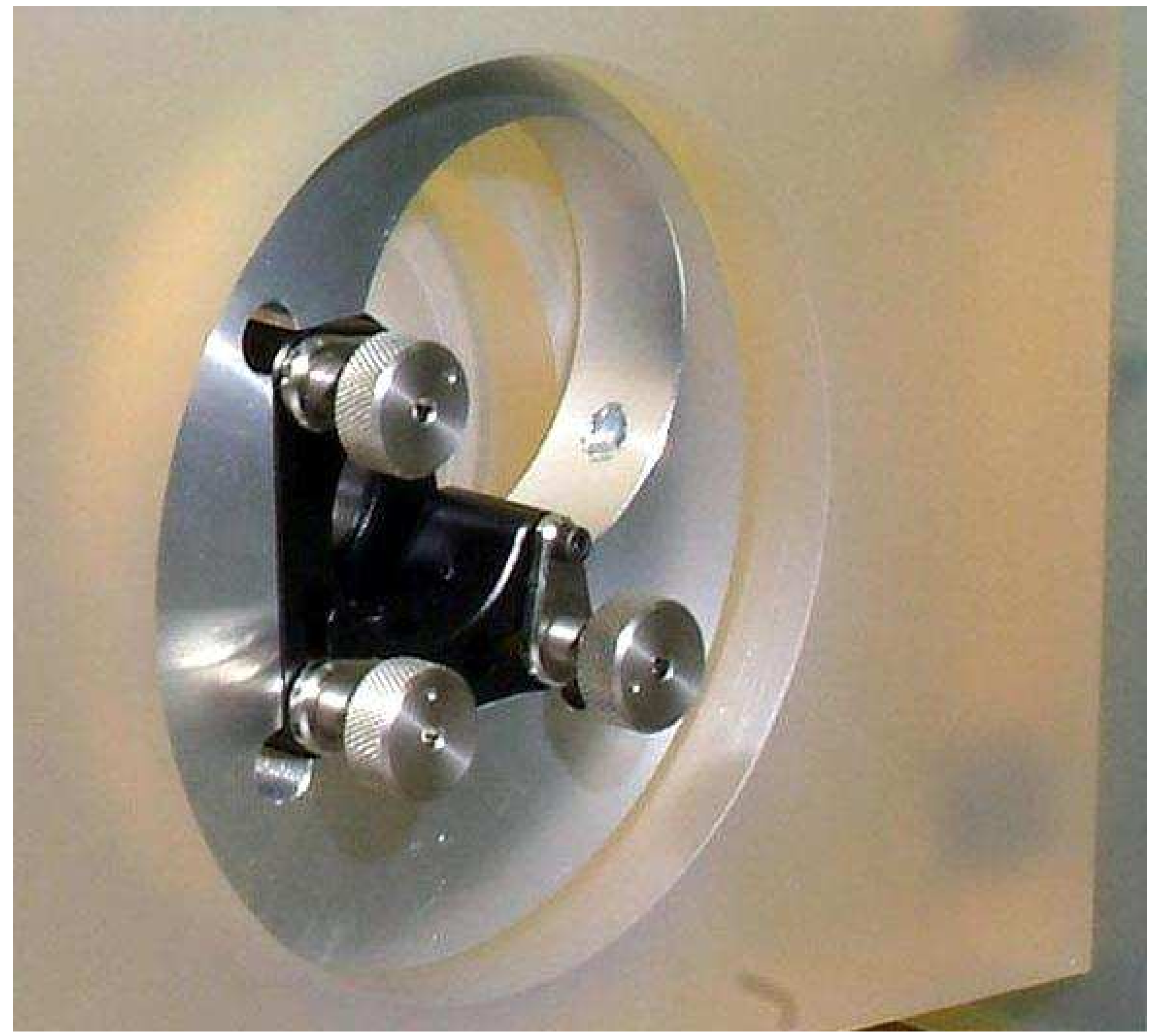

An attempt to glue the Zerodur mirrors to the Zerodur baseplate failed: Curing of the glue caused $\approx 200\,\mu$rad misalignment and a contrast drop to < 0.5. This is mainly a testing problem.

EM Test results: Noise sources 3

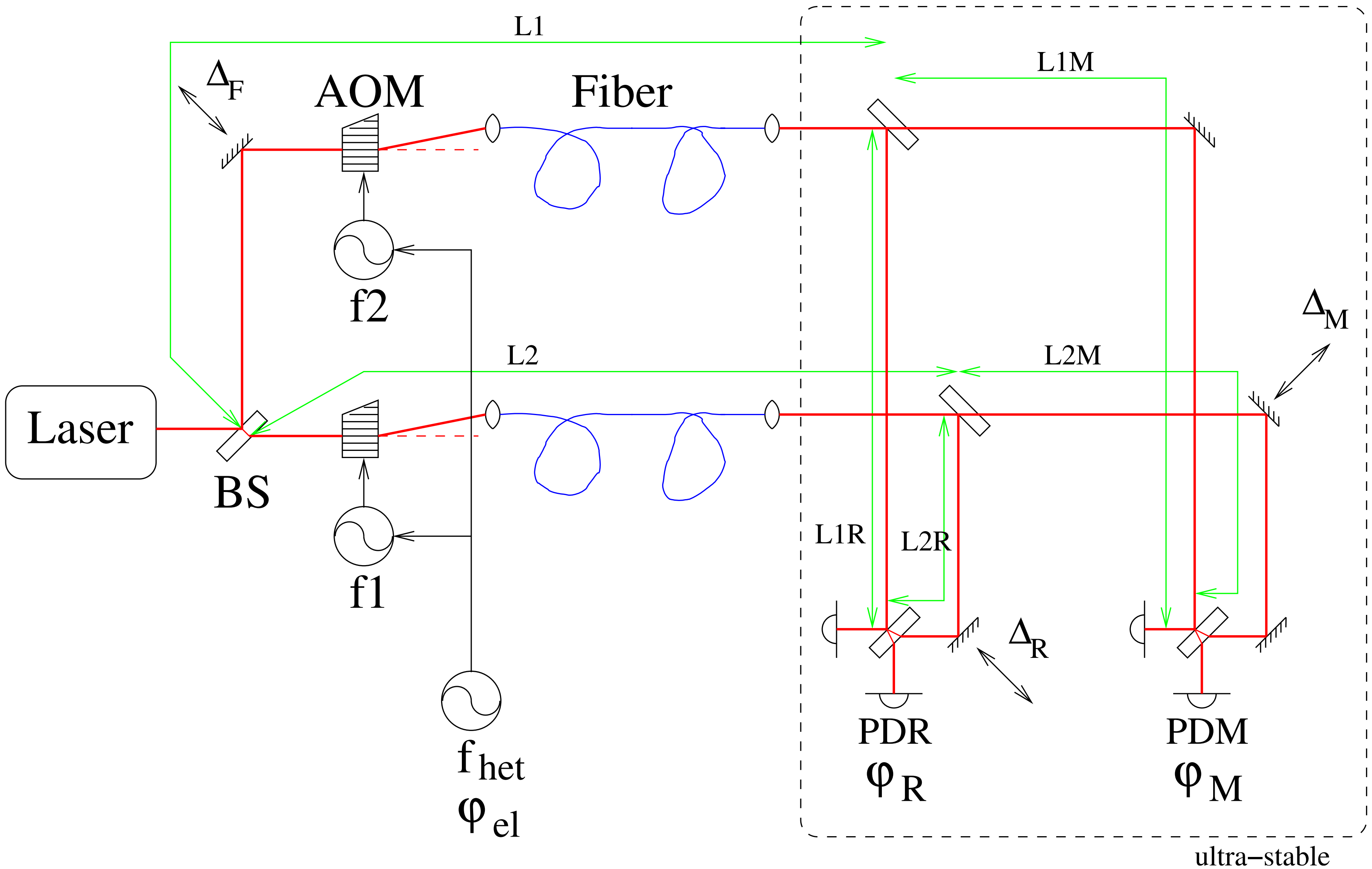

Fluctuations of the fibers' Optical Pathlength Difference (OPD, Δ_F) should ideally completely cancel, but in reality some error remains.

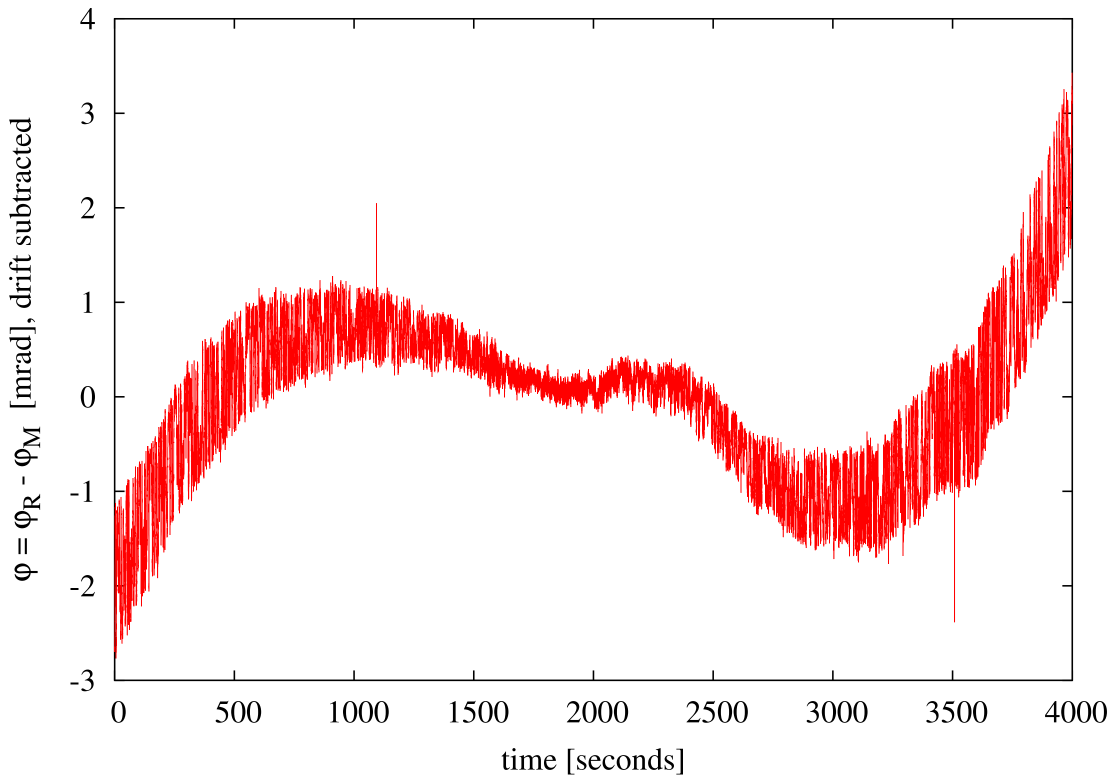

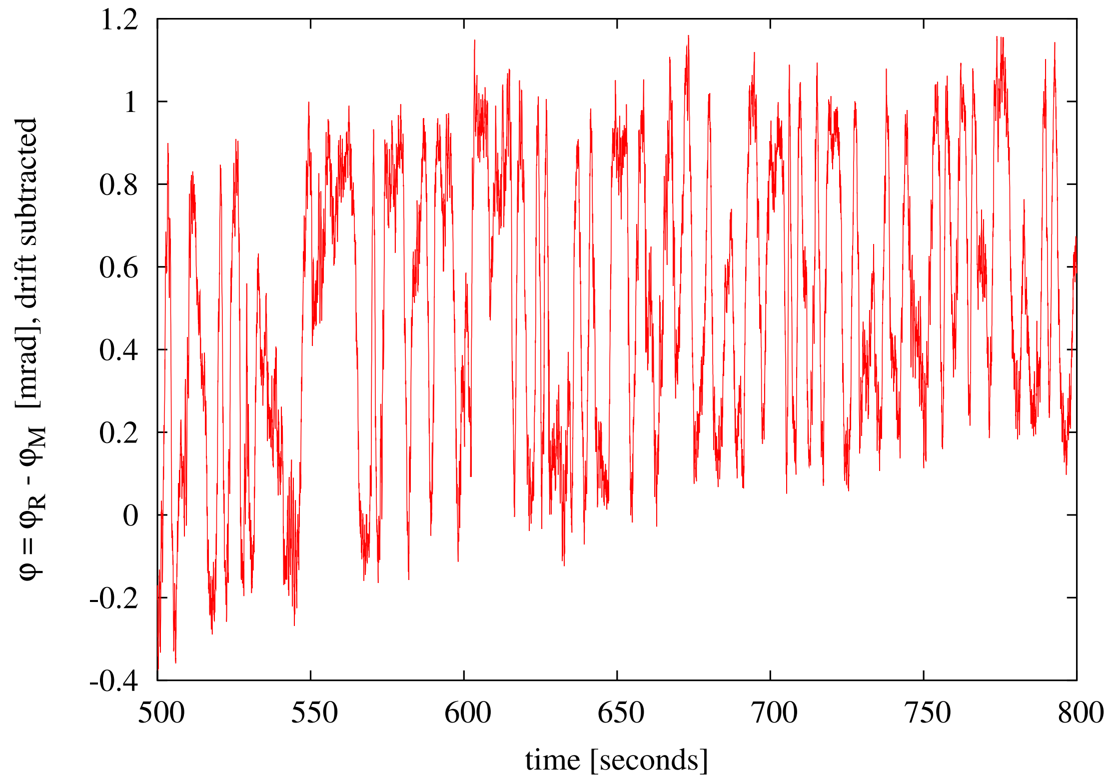

The measured pathlength $x_1 - x_2$ signal has an erroneous component of $\approx$ mrad magnitude which is quasi-periodic with Δ_F.

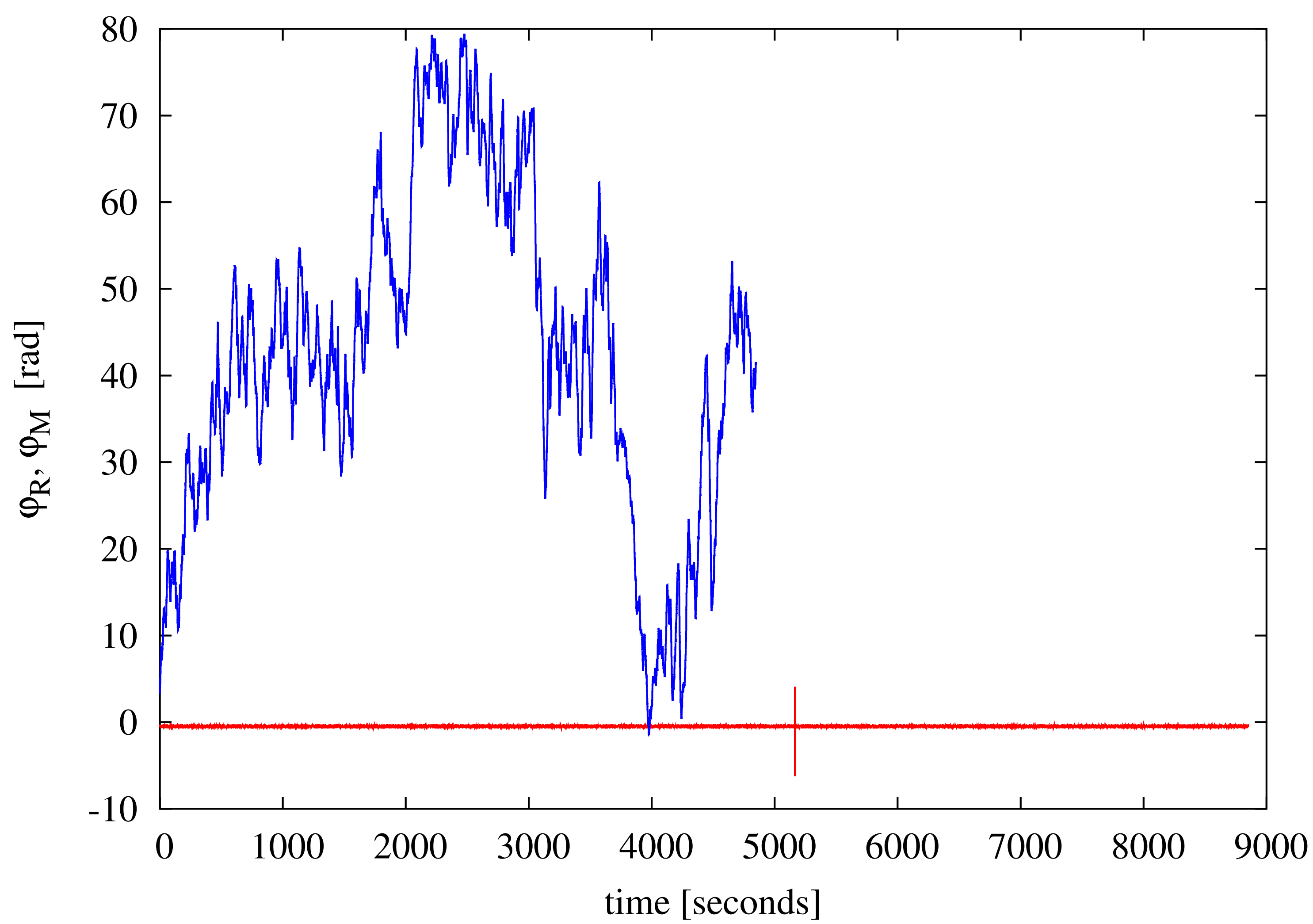

Unless the origin of the noise will be understood, a remedy is to actively stabilize Δ_F. This was done using an analog phasemeter, analog servo and long-range PZT at TNO.
Further investigations are under way in Hannover and Glasgow.

Alignment measurement with quadrant photodiodes

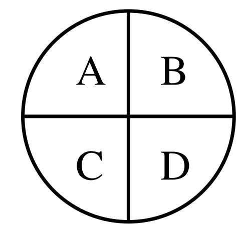

3 ways to use a quadrant diode:

- $\Sigma = A + B + C + D$ is used as before for the longitudinal readout.

- The DC signals $\Delta y = A + B - C - D$ and $\Delta x = A + C - B - D$ measure the **average lateral displacement** of both beams.

- Differential wavefront sensing measures the **angle between interfering wavefronts:**

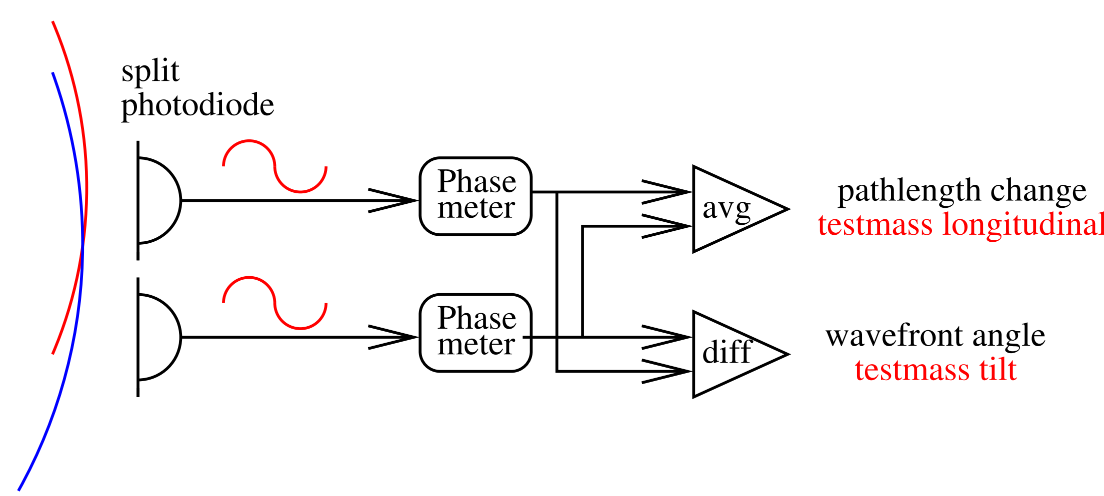

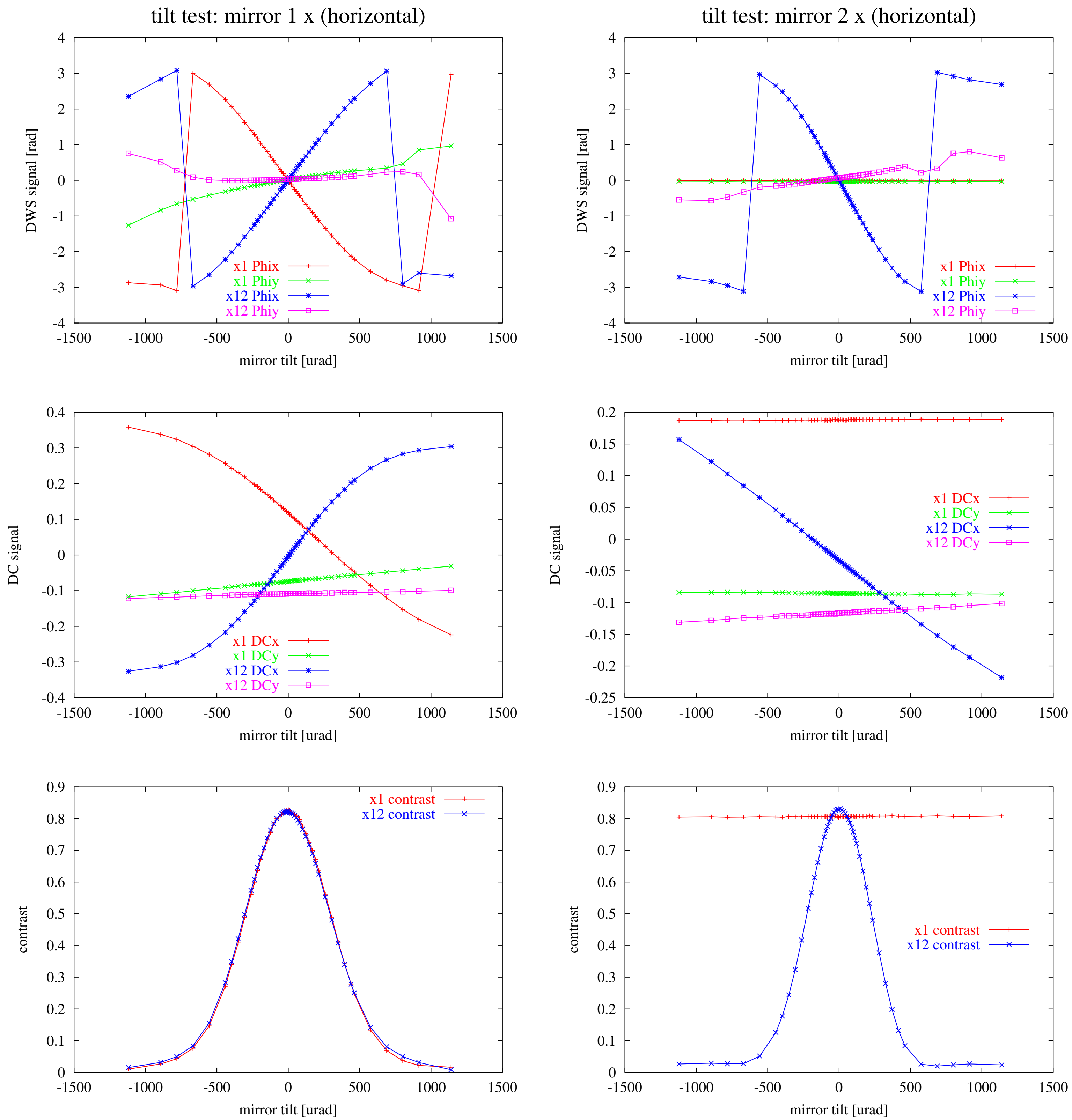

tilt test: mirror 1 x (horizontal)
tilt test: mirror 2 x (horizontal)
DWS signal [rad]
mirror tilt [urad]
x1 Phix
x1 Phiy
x12 Phix
x12 Phiy
DC signal
x1 DCx
x1 DCy
x12 DCx
x12 DCy
contrast
x1 contrast
x12 contrast

EM Test results: Differential wavefront sensing (DWS)

The conversion factor of test-mass angle α to (differential) phase readout φ is analytically:

$$\varphi/\alpha = 2\sqrt{2\pi}w(z)/\lambda \approx 5000\,\text{rad/rad}.$$

	Rot. TM1	Rot. TM2	units
x_1 ifo predicted (numerical)	5337	0	rad/rad
x_1 ifo measured (x)	5441	0	rad/rad
x_1 ifo measured (y)	5167	0	rad/rad
$x_1 - x_2$ ifo predicted (numerical)	4963	5994	rad/rad
$x_1 - x_2$ ifo measured (x)	5365	7263	rad/rad
$x_1 - x_2$ ifo measured (y)	5072	6940	rad/rad

- conversion factor depends on beam parameters; calibration is necessary.

- Better than the angular readout capability of the capacitive sensors; will be used to stabilize the alignment of the test masses.

- DWS works only when there are fringes (test mass absolute alignment better than 300 μrad). Otherwise, DC alignment signals are used for rough alignment of test mass.

EM Test results: Differential wavefront sensing (DWS)

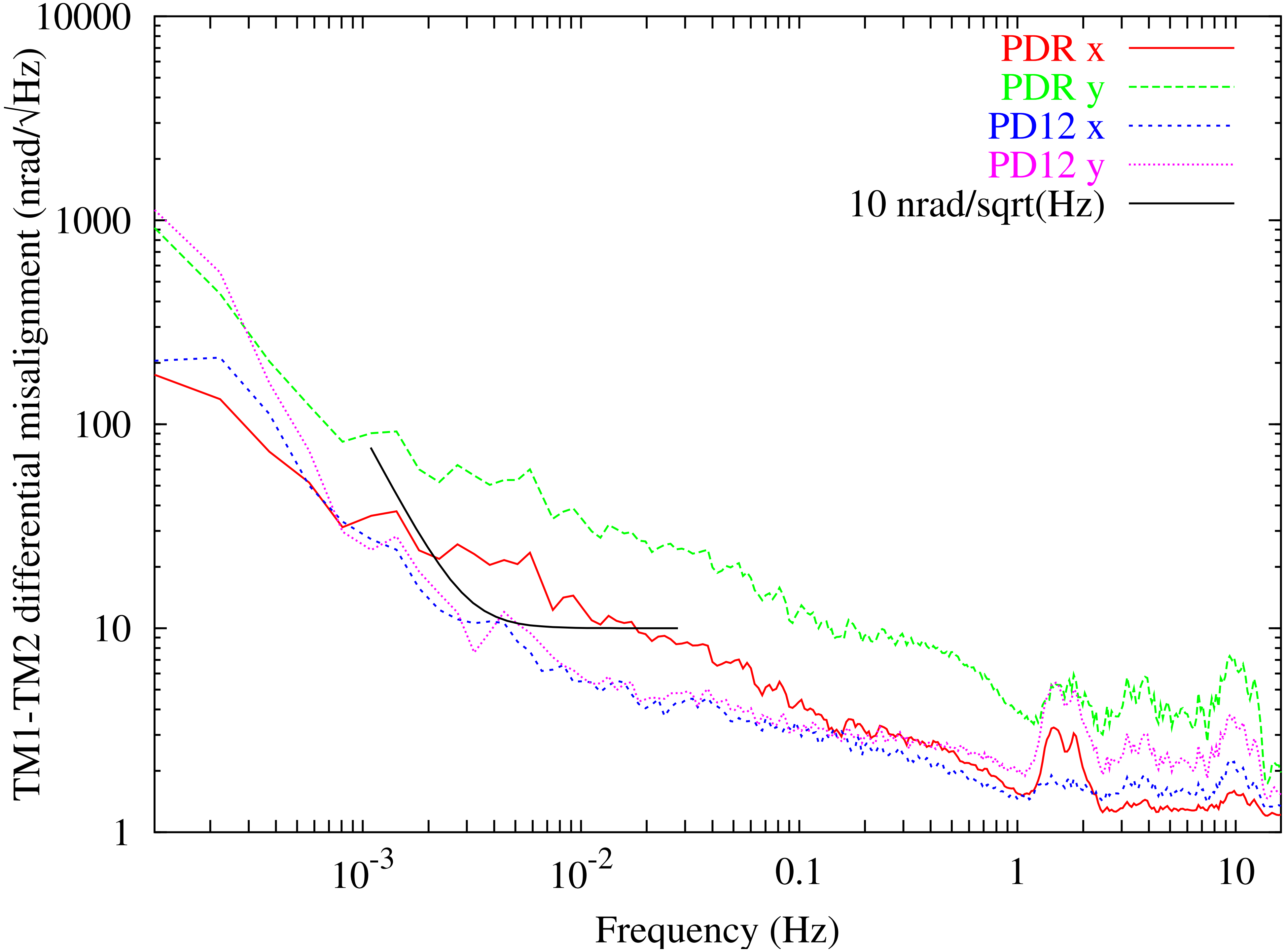

Summary

- interferometry and phase measurement for LTP work as predicted.
- some minor refinements are needed in the construction procedure.
- environmental and performance testing was successful.
- Optical pathlength difference (OPD) must be stabilized to reach performance goal.
- Open question: performance impact of optical window.
- Open question: caging mechanism!